MICROCOPY RESOLUTION TEST CHART

NATIONAL BUREAU OF STANDARDS

AFWAL-TR-84-4062

EVALUATION OF COD COMPLIANCE
DETERMINED CRACK GROWTH RATES

D. C. Maxwell
J. P. Gallagher
N. E. Ashbaugh

UNIVERSITY OF DAYTON
RESEARCH INSTITUTE
300 COLLEGE PARK DRIVE
DAYTON, OHIO 45469

JUNE 1984

INTERIM REPORT FOR PERIOD NOVEMBER 1981 - JANUARY 1983

THEODORE NICHOLAS, Project Engineer
Metals Behavior Branch

JOHN P. HENDERSON. Chief
Metals Behavior Branch
Metals and Ceramics Division

FOR THE COMMANDER

GAIL E. EICHELMAN, Act'g Chief
Metals and Ceramics Division
Materials Laboratory

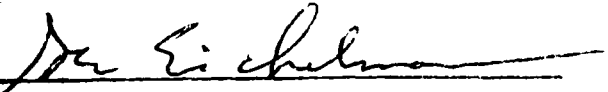| REPORT DOCUMENTATION PAGE		READ INSTRUCTIONS BEFORE COMPLETING FORM
1. REPORT NUMBER AFWAL-TR-84-4062	2. GOVT ACCESSION NO. AD·H144037	3. RECIPIENT'S CATALOG NUMBER
4. TITLE *(and Subtitle)* EVALUATION OF COD COMPLIANCE DETERMINED CRACK GROWTH RATES		5. TYPE OF REPORT & PERIOD COVERED Interim Report Nov. 1981 – Jan. 1983
		6. PERFORMING ORG. REPORT NUMBER
7. AUTHOR(s) D. C. Maxwell J. P. Gallagher N. E. Ashbaugh		8. CONTRACT OR GRANT NUMBER(s) F33615-81-C-5015
9. PERFORMING ORGANIZATION NAME AND ADDRESS University of Dayton Research Institute 300 College Park Drive Dayton, Ohio 45469		10. PROGRAM ELEMENT, PROJECT, TASK AREA & WORK UNIT NUMBERS P.E. 61102F 2307-P1-14
11. CONTROLLING OFFICE NAME AND ADDRESS Materials Laboratory (AFWAL/MLLN) Air Force Wright Aeronautical Laboratories Wright-Patterson AFB, Ohio 45433		12. REPORT DATE June 1984
		13. NUMBER OF PAGES 58
14. MONITORING AGENCY NAME & ADDRESS*(if different from Controlling Office)*		15. SECURITY CLASS. *(of this report)* Unclassified
		15a. DECLASSIFICATION DOWNGRADING SCHEDULE

16. DISTRIBUTION STATEMENT *(of this Report)*

Approved for public release; distribution unlimited.

17. DISTRIBUTION STATEMENT *(of the abstract entered in Block 20, if different from Report)*

18. SUPPLEMENTARY NOTES

19. KEY WORDS *(Continue on reverse side if necessary and identify by block number)*

fatigue crack growth rate
non-visual crack length measurement
X7091 aluminum
modulus

stress intensity factor
crack-opening-displacement
compliance

20 ABSTRACT *(Continue on reverse side if necessary and identify by block number)*

Fatigue crack growth rate studies were conducted on sixteen X7091 aluminum specimens. Crack growth rates were determined by visual crack length measurements and crack-opening-displacement (COD) compliance measurement. The curves of crack growth rate versus stress intensity factor from COD compliance measurements were compared to the optical crack growth rate results which were determined by following ASTM E647 Standard Test Method for Constant-Load-Amplitude Fatigue Crack Growth Rates Above 10^{-8} m/Cycle. Differences between

the growth rates from the two methods are discussed in terms of potential errors in the evaluation of variables used in the data collection and analysis.

The use of a "handbook" elastic modulus value has been found to be a source of significant error. The use of an "effective" modulus value calculated from the initial visual crack length is recommended.

FOREWORD

This interim report was prepared by the University of
Dayton Research Institute under Contract No. F33615-81-C-5015.
It was administered under the direction of the Materials
Laboratory, Air Force Wright Aeronautical Laboratories, Wright-
Patterson Air Force Base, Ohio with Dr. T. Nicholas as Project
Monitor.

This report describes one of the work activities covered
under Task 2 of the contract. The work described herein was
conducted between November 1981 and January 1983. Various
individuals contributed to the development of the tests and the
data reduction. Mr. D. Maxwell was responsible for the
coordination of all the activities reported. Drs. T. Weerasooriya
and A. M. Brown advised Mr. Maxwell on the test set up and the use
of the ASTM E647-81 Method of Test. Mr. D. Roalef assisted in
precracking and in conducting the tests. Ms. Elizabeth Dirkes
assisted in data reduction and plotting.

Accession For

NTIS GRA&I   X
DTIC TAB   ☐
Unannounced   ☐
Justification _____

By _____
Distribution/
Availability Codes
         Avail and/or
Dist   Special

A-1

iii

TABLE OF CONTENTS

PREVIOUS PAGE
IS BLANK

LIST OF FIGURES

LIST OF FIGURES (Concluded)

LIST OF TABLES

SECTION 1

INTRODUCTION

The present technology for fatigue crack growth rate testing of metals generally employs visual examination of the fatigue crack to determine crack extension between applied load cycles. Visual examination requires personal supervision, specimen surface preparation for crack tip enhancement, and an adequate optics system for accurate crack length measurements. The accuracy of fatigue crack growth rate data is dependent upon the attention given to each of the above mentioned elements in the measurement system. The need for consistently accurate measurements and less manpower dependence necessitates the use of an automated data acquisition system. One method of automated data acquisition makes use of compliance measurements. The compliance is the inverse stiffness of the specimen and changes as a function of crack length as illustrated in Figure 1.

In a previous investigation[1]*, the University of Dayton Research Institute (UDRI) characterized the fatigue crack growth properties of Rapid Solidification Technique (RST) P/M Aluminum X7091. In these tests, visual crack growth measurements were collected and load-displacement plots were recorded. Fatigue crack growth rate data (da/dN versus ΔK) were generated using the visual measurement data. The tests were conducted in accordance with ASTM E647-81 Test Method[2] for Constant-Load-Amplitude Fatigue Crack Growth Rates Above 10^{-8} m/cycle.

The purpose of this report is to evaluate fatigue crack growth rates generated from COD compliance measurements. The compliance data from the X7091 Aluminum crack growth study are reduced to generate da/dN versus ΔK curves which are compared

---

*Superscript numbers refer to literature citations, see list of references.

1
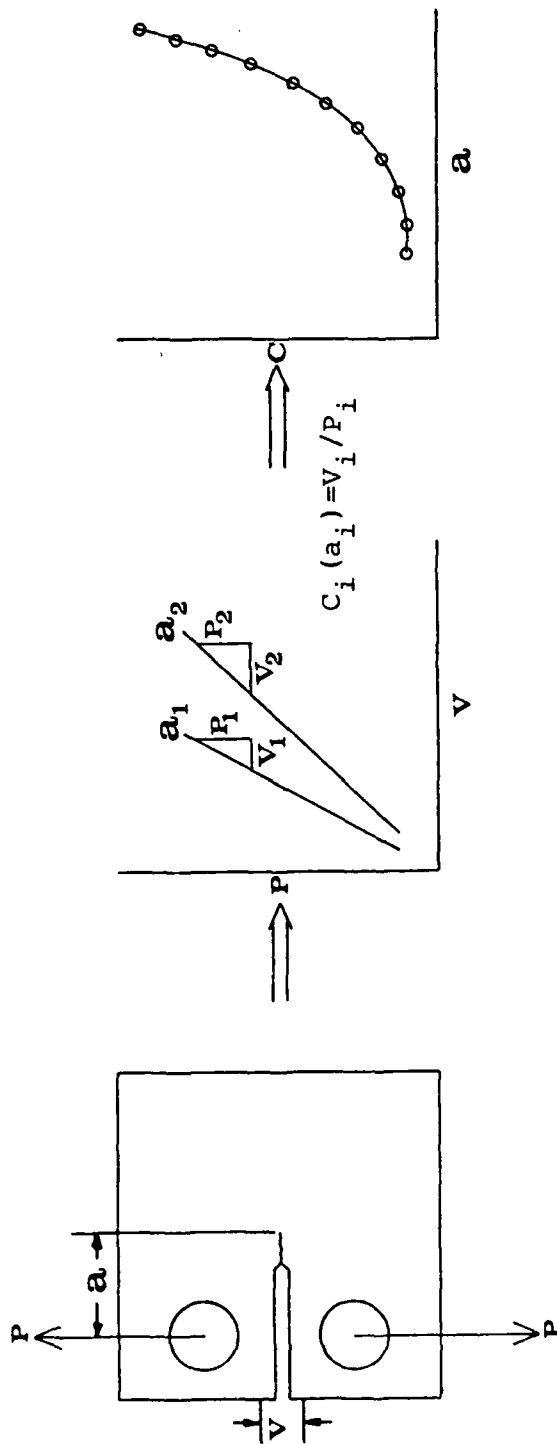
Figure 1. Relationship Between Compliance and Crack Length.

$$C_i(a_i) = V_i/P_i$$

to the da/dN versus ΔK curves generated from the visual measurement data. Differences between the resulting crack growth rate curves and reasons for these differences are discussed. Recommendations are made concerning the use of compliance to generate fatigue crack growth rate data.

SECTION 2
TEST METHODS

2.1 SPECIMEN GEOMETRY AND LOADING CONDITIONS

The fatigue crack growth rate tests were conducted using a standard compact tension specimen with a width (W) of 2.0 inches and a thickness (B) of 0.25 inch. The specimen geometry conformed to ASTM Method E647-81 (Figure 2). Each test specimen was measured on a Gaertner Machinist's microscope equipped with a Gaertner Digital Readout System. See Table 1 for a summary of specimen dimensions.

The specimens were precracked on a 20,000 pound MTS materials testing machine at a frequency of 20 Hz. The precracking was started at a load between 600 and 800 pounds and a stress ratio (R) of 0.1; after crack initiation, the loads were progressively lowered until a crack growth rate of less than 4×10^{-7} inches/cycle was achieved. The stress ratio was increased to 0.3 before the completion of precracking. The fatigue crack growth rate tests were conducted on a 10,000 pound MTS materials testing machine under constant amplitude load. The test conditions were such that the maximum load was set at a level 20 pounds above the last precracking load and the stress ratio was 0.3.

The frequency at the start of all tests was set at 20 Hz. To obtain the load-displacement data required for compliance analysis, the frequency was reduced to 0.5 Hz for several cycles so that the load-displacement data could be recorded using an X-Y plotter. When the frequency was periodically lowered to 0.5 Hz, the load was noted to increase which could result in a possible overload condition. To prevent an overload, the MTS load controls were readjusted. The loading conditions for each test are summarized in Table 2.

As the crack grew and the displacement increased, it was also necessary to adjust the MTS load controls to maintain the prescribed load parameters. To minimize the change in load

4
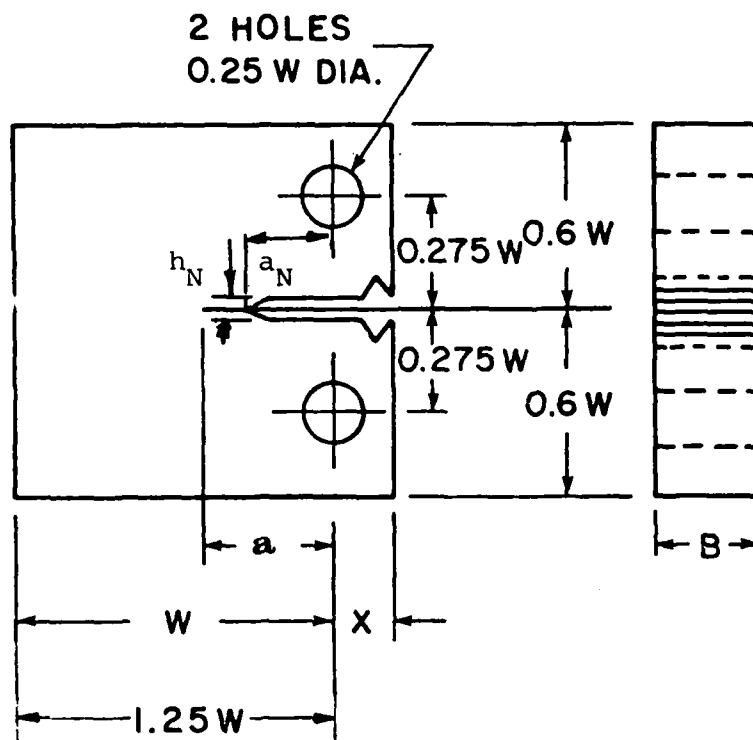
Figure 2. Compact Tension Specimen for Fatigue Crack Growth
Rate Testing (See Table 1 for Physical Measurements).

TABLE 1

SUMMARY OF SPECIMEN DIMENSIONS

Specimen Number	Thickness (B) (Inches)	Width (W) (Inches)	Notch Height (hN) (Inches)	Notch Length (aN) (Inches)	0.2% Offset Yield Strength* (ksi)
CTX4	0.2466	1.9999	0.093	0.4983	78.7
CTX32	0.2468	1.9828	0.093	0.4960	79.8
CT331	0.2459	2.0004	0.094	0.5008	--
CT472	0.2433	1.9999	0.095	0.5004	73.7
FC41	0.2518	1.9882	0.094	0.5046	77.5
FC42	0.2453	1.9801	0.093	0.5115	67.5
FC61	0.2512	2.0024	0.094	0.5056	73.4
FC71	0.2505	1.9887	0.098	0.5033	69.4
FC91	0.2506	1.9985	0.094	0.5089	18.1 (sic)
SMA1	0.2520	1.9925	0.094	0.5008	79.1
SME	0.2515	1.9944	0.096	0.5109	77.9
SM1TF	0.2520	2.0032	0.095	0.5069	75.3
SM3TF	0.2519	1.9989	0.101	0.5064	70.0
SM6TF	0.2514	1.9998	0.095	0.5043	70.4
SM8TF	0.2496	1.9965	0.072	0.4977	70.9
SM8TS2	0.2533	2.0036	0.096	0.5064	--

*The 0.2% Offset Yield Strength Values were provided by Met-Cut on the same batch of material.

6

TABLE 2

SUMMARY OF TEST CONDITIONS

	PRECRACKING LOAD CONDITION		TEST CONDITIONS		
Specimen Number	Initial P_{Max} (Pounds)	Minimum Acceptable Crack Length (Inches)	P^{*}_{Max} (Pounds)	a_o (Inches)	a_f (Inches)
CTX4	600	.5913	270	0.5444+	1.5823
CTX32	600	.5890	270	0.6132	1.4732
CT331	600	.5948	270	0.8501	1.4623
CT472	600	.5954	270	0.5387+	1.5024
FC41	800	.5986	420	0.6095	1.4148
FC42	600	.6045	270	0.6064	1.5277
FC61	600	.5996	350	0.6664	1.4956
FC71	600	.6023	270	0.5533+	1.5143
FC91	.600	.6029	295	0.6095	1.4790
SMA1	800	.5968	270	0.5896+	1.4667
SME	800	.6069	370	0.6840	1.4811
SM1TF	800	.6019	450	0.6545	1.1591
SM3TF	800	.6074	345	0.6231	1.5048
SM6TF	800	.5993	520	0.5661+	1.3573
SM8TF	600	.5697	450	0.6083	1.4389
SM8TS2	700	.6024	370	0.5856+	1.4997

*Stress Ratio was 0.3 for all tests.

+ a_o < a_{min} per ASTM E647.

7

controls, the testing frequency for some tests was gradually reduced from 20 Hz to 5 Hz as the displacement increased.

2.2   VISUAL CRACK LENGTH MEASUREMENTS

The crack length was monitored on both sides of the specimen, using microscopes mounted on micrometer slides equipped with digital readouts. Crack length measurements were scheduled to be made after approximately every 0.020 inches of crack growth. Actual measurements were made after every 0.018 ± 0.006 inches of crack growth. ASTM E647-81 Test Method required crack length measurements to be made every 0.040 inches for $a/W \leq 0.60$ and 0.020 inches for $a/W > 0.60$. Accuracy of the visually measured crack length extensions was ± 0.002 inches; well within ± 0.004 inches as recommended in ASTM E647-81 Test Method.

The fatigue crack was to be extended to approximately one inch beyond the notch tip, but several tests were discontinued sooner because of significant yielding at the crack tip or because the fatigue crack tip had departed from the plane of symmetry by more than ± 5 degrees which was measured from the notch root. The average initial (a_o) and final (a_f) crack lengths between which crack growth data were collected for each specimen can be found in Table 2.

UDRI was requested to begin collecting fatigue crack growth data after a precrack length of 0.030 to 0.050 inches (as measured from the notch) had been attained. ASTM Method E647-81 requires a minimum fatigue precrack of 0.1B (specimen thickness) or h_N (notch height), whichever is greater (see Table 1 for B and h_N dimensions). A precrack length of 0.030 to 0.050 inches does not meet this requirement and all data recorded before the minimum fatigue crack length listed in Table 2 are considered invalid data and were disregarded for subsequent analysis.

8

Although the specimen thickness is such that the fatigue crack length measurements are required on only one side, measurements were made on both the front and back sides of the specimen. The average value of these measurements was used in the calculations. The ASTM standard indicates that data are invalid where the two crack lengths at a given number of cycles differ by more than 0.025W or 0.25B, whichever is less. Whenever the difference in the two crack lengths exceeded the allowable tolerances, the specimen grips were clamped on the longer crack length side in an attempt to bring the crack length differential into tolerance. On several specimens, it was not possible to obtain a valid crack length differential; these data are therefore invalid according to ASTM E647-81 Test Method. The data (a vs N) collected either under the clamping conditions or where front and back crack lengths differed more than the ASTM E647 requirements were not utilized for any da/dN calculations.

2.3 COMPLIANCE MEASUREMENTS

A crack opening displacement (COD) technique was used to determine specimen compliance. Compliance is the crack opening displacement per unit load. The crack opening displacement was measured at the front face of the specimen (one half inch from the load line). The crack opening displacement and load were autographically plotted after approximately every 0.100 inches of crack growth. Figure 3 shows typical load-displacement curves exhibited during the test program.

The load versus crack opening displacement curves were evaluated to determine the compliance values. Compliance - the inverse of the slope - was determined by visually fitting a straight line to the upper linear portion of the loading curve as illustrated in Figure 3. The typical type of load-displacement behavior with slight nonlinearity at low loads is illustrated in Figure 3a. Several specimens exhibited the more extreme nonlinear behavior on the lower portion of the COD curves as shown in Figure 3b. This behavior was possibly caused by internal

9
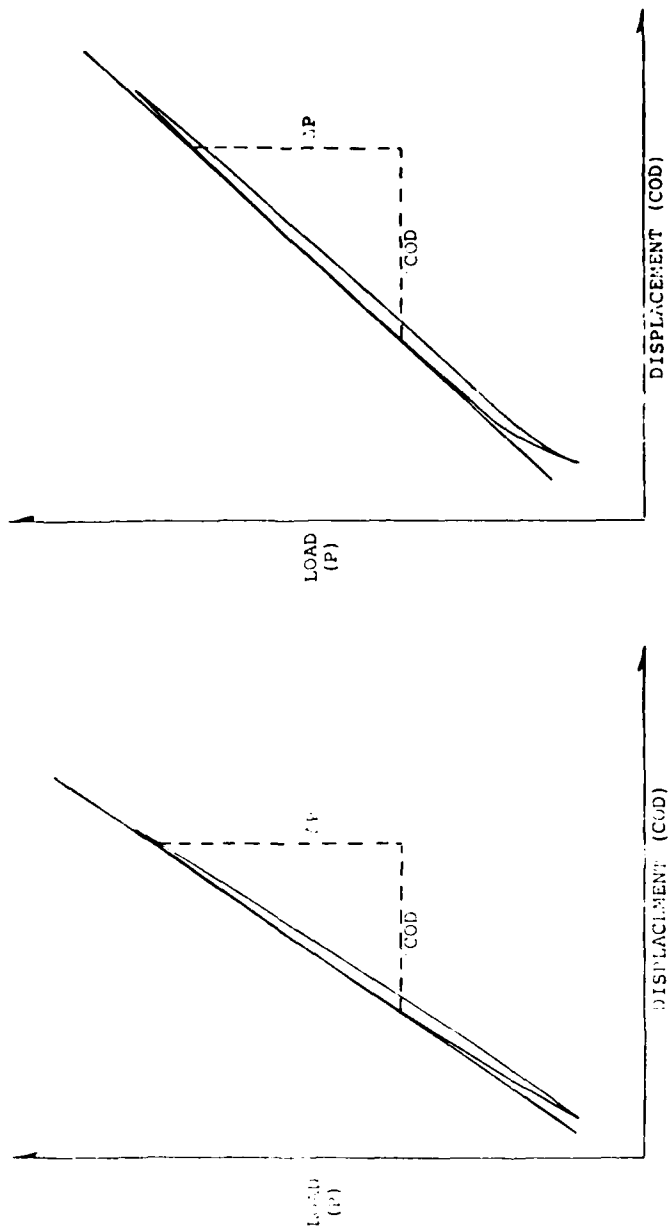
a. Typical Behavior   b. Atypical Behavior

Figure 3. Schematic Illustration of Types of Load (P) Versus Displacement (COD) Behaviors Exhibited During the Test Program.

10

(residual) stresses that resulted from the heat treating process or that were generated by the fatigue crack growth process. The compliance was determined on that linear portion of the curve above the initial nonlinear behavior. Typically, the linear portion occurred between 30-90% of maximum load.

The crack opening displacement was measured using a double-cantilever displacement gage with a sensitivity of 0.002 inches/volt and an accuracy of ± 0.5 percent of full scale or ± 0.0001 inches over a 0.02 inch range. The load was measured on the 1,000 pound range of a 10,000 pound MTS load cell with an accuracy of ± 0.5 percent of range. Repeated measurements of the slope of a load-displacement curve did not vary more than ± 2 percent. When all systematic and random errors were taken to their limit, the maximum error in compliance could be five percent.

SECTION 3
DATA REDUCTION

3.1   VISUAL CRACK GROWTH RATE

The crack length versus elapsed cycles (a versus N) were used to determine the rate of fatigue crack growth. The data were reduced using the seven point incremental polynomial technique as described in ASTM E647-81 Test Method. This technique numerically "smooths" the data by fitting a second-order polynomial to sets of seven successive data points.

The rate of crack growth at N_i, the middle cycle count value, is obtained from the derivative of the second-order polynomial, which is given by the following expression:

$$(da/dN)_{\hat{a}_i} = \frac{b_1}{C_2} + 2b_2 \ (N_i - C_1)/C_2^2 \tag{1}$$

The value of ΔK associated with this da/dN value is computed using the crack length, $\hat{a}_i$, obtained from the second-order polynomial expression evaluated at N_i.

3.2   COMPLIANCE CRACK GROWTH RATE

Mathematical expressions for the determination of crack length have been formulated for various displacement-measurement locations on the specimen. The displacement-measurements reported for this test series were recorded for a location that had a distance in front of the load line (X) to specimen width (W) ratio of -0.25 (Figure 2). For X/W = -0.25, crack length is a function of compliance as expressed by the formula[3]

$$\alpha = \frac{a}{W} = 1.0010 - 4.6695U^{-1} + 18.46oU^{-2} - 236.82U^{-3}$$
$$+ 1214.9U^{-4} - 2143.6U^{-5} \tag{2}$$

12

where $U = (\frac{EBV}{P})^{\frac{1}{2}} + 1 = (EBC)^{\frac{1}{2}} + 1$ (2a)

and where

     a = Crack Length (inches)

     W = Specimen Width (inches)

     B = Specimen Thickness (inches)

     E = Elastic* Modulus (psi)

     V = Crack Opening Displacement (inches)

     P = Load (pounds)

     C = V/P = Compliance (inches/pound)

The crack growth rates associated with the compliance measurements were calculated using the secant method described in the ASTM E647-81 Test Method. The difference in crack lengths (Δa) for the calculations was obtained from the successive compliance calculated crack lengths and the difference in cycles (ΔN) was obtained from the respective cycle count at which the compliance calculations were taken, i.e.,

$$\left(\frac{da}{dN}\right)_{\bar{a}} = \frac{\Delta a}{\Delta N} = \frac{a_{comp_2} - a_{comp_1}}{N_2 - N_1} \quad\quad (3)$$

The average crack length ($\bar{a}$) obtained from successive compliance measurements was used to calculate the corresponding ΔK value (see Figure 4).

---

*Plane stress or plane strain conditions as appropriate.
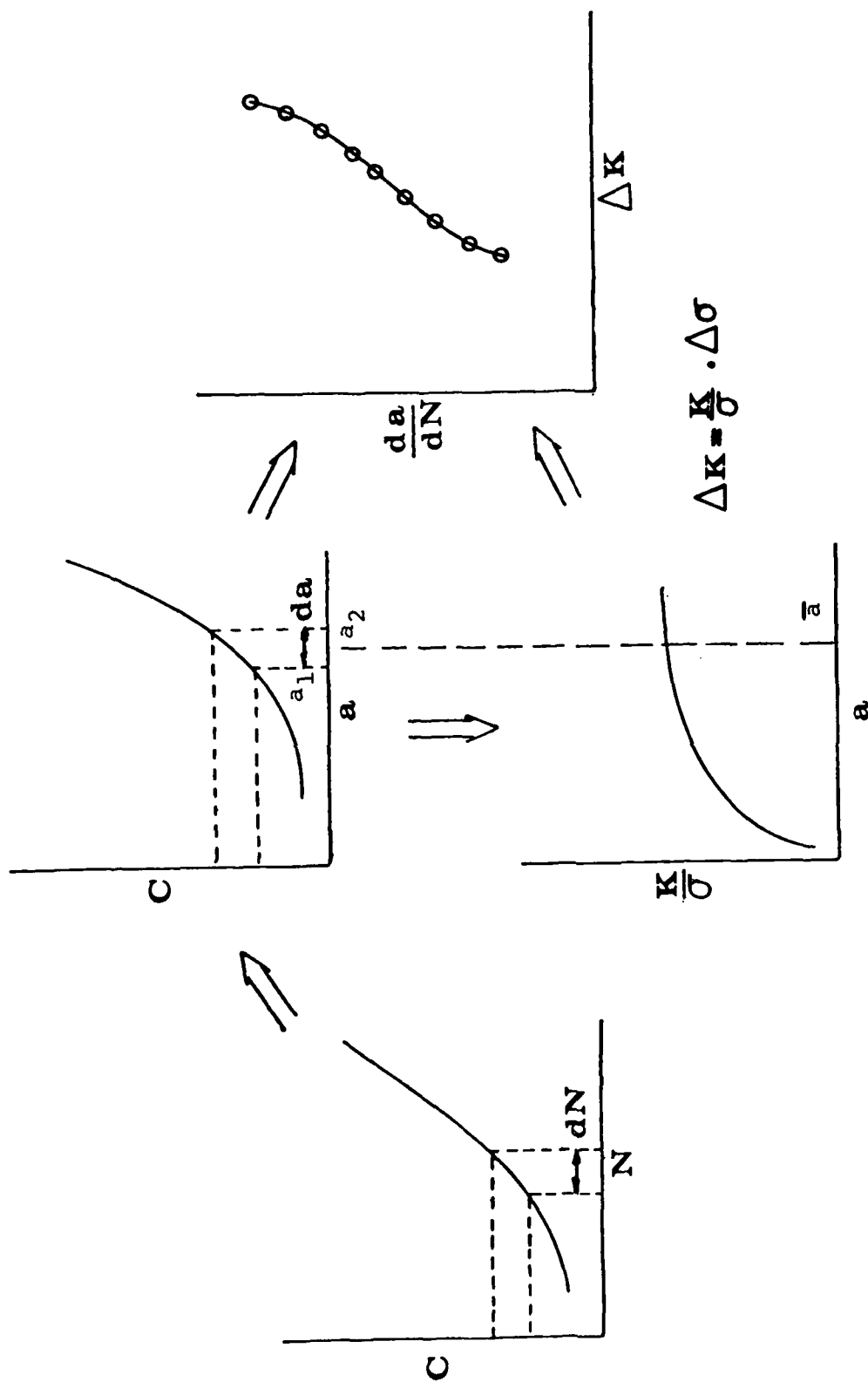
$$\Delta K = \frac{\Delta P}{BVW} \frac{(2+\alpha)}{(1-\alpha)^{3/2}} (0.886 + 4.642\alpha - 13.32\alpha^2 + 14.72\alpha^3 - 5.6\alpha^4) \quad (4)$$

WHERE $\alpha = \frac{a}{W}$

Figure 4. Nonvisual Method of Determining Crack Growth Rate.

14

SECTION 4
RESULTS AND DISCUSSION

4.1 INITIAL DATA REDUCTION AND COMPARISON

In Equation 2, all the parameters are either measured
prior to the test or monitored during the course of the test
except E, the modulus. The modulus employed to make these cal-
culations was a "handbook" value, 10.6×10^6 psi. Using Equation
3 in conjunction with Equation 2 resulted in the compliance
determined crack growth rates shown in Figure 5. The crack growth
rate data obtained from visual measurements using the seven-point
polynomial incremental step method are also included. A compari-
son of the visual and compliance results indicates that the
growth rates have a similar trend but one is shifted relative to
the other. The visual data are assumed to reflect the correct
crack growth behavior since the ASTM E647-81 Test Method was
followed.

The three crack growth rate data sets chosen for presen-
tation in Figure 5 show distinctively that the compliance
determined crack growth rates differ significantly from the
visual seven-point polynomial based rates. The crack growth rate
data from the other 13 specimens are summarized in Figures A1
through A13 of the Appendix. Of the 16 data sets, the three sets
in Figure 5 exhibited the greatest difference between the two
methods of obtaining crack growth rate behavior. While the other
13 data sets showed better agreement between the two crack growth
rate methods, the compliance results generally were above the
visual results. It was decided that an improvement in the
compliance method was required before it could be accepted for
calculating crack growth rates. A study was therefore conducted
to evaluate the effect of potential errors in the compliance
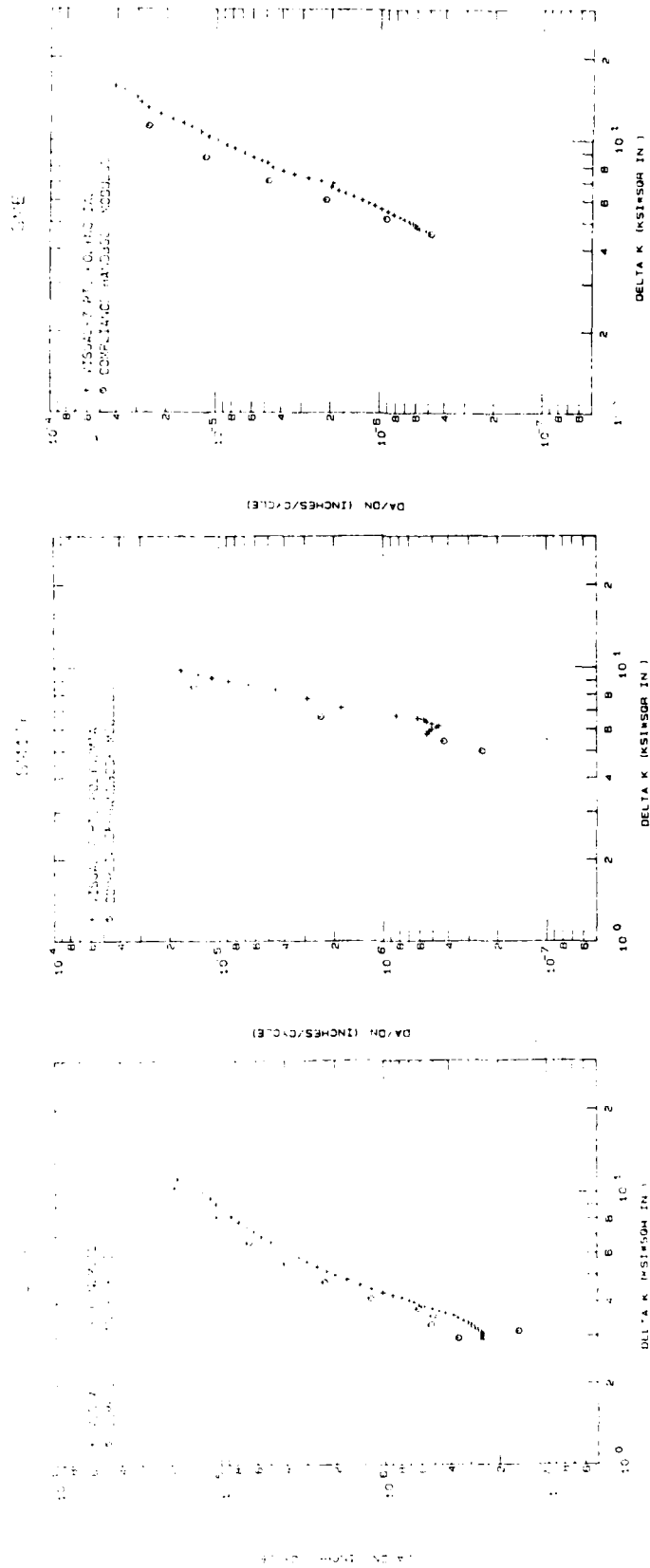method on crack growth rate results.

15

Figure 5. Comparison Between Compliance Based Crack Growth Rates (Secant Method) and Visual Crack Growth Rates (7-Point Polynomial). Compliance Determined Crack Lengths Based on Handbook Elastic Modulus Value of 10.6x106 psi.

16

4.2   THE IMPACT OF POTENTIAL ERRORS

The impact of potential errors in compliance calculated crack growth rate behavior can be analyzed using the non-dimensional compliance parameter EBC given in Equation 2a. Figures 6, 7, and 8 describe the effect that ±1, ±5, and ±10 percent errors in EBC can have on the errors in the compliance calculated crack length, (a), in its associated stress-intensity factor range, (ΔK), and in the incremental extension, (Δa), of compliance calculated crack length, respectively.

Figure 6 shows the impact of a fixed percent error in EBC which results in rapidly decreasing percent errors in the estimated value of crack length as the crack length increases. It is noted that the maximum percent error in estimated crack length over the range of interest is only slightly larger than the percent error in EBC.

Figure 7 shows the effect of percent errors in EBC on the percent error in the stress-intensity factor range (ΔK). It is seen that the percent error in ΔK is almost independent of crack length for a fixed error in EBC. The reason for the crack length independence behavior shown in Figure 7 can be obtained through a coupling of Figure 6 results with an analysis of the impact of crack length errors on the error in ΔK. Figure 9 describes the results of the latter analysis; note that the percent errors in ΔK increase exponentially as a function of crack length. Figure 7 also shows that the percent error in ΔK is approximately the same as (but less than) the percent error in EBC.

Figure 8 shows the effect of percent errors in EBC on the percent error in the crack growth increment. The errors in Δa were calculated for approximately 0.1 inch increment of crack growth which were measured experimentally. The error was plotted in Figure 8 as a function of the mean crack length for that increment. Additional calculations of errors were determined for arbitrarily small values of Δa. These limiting
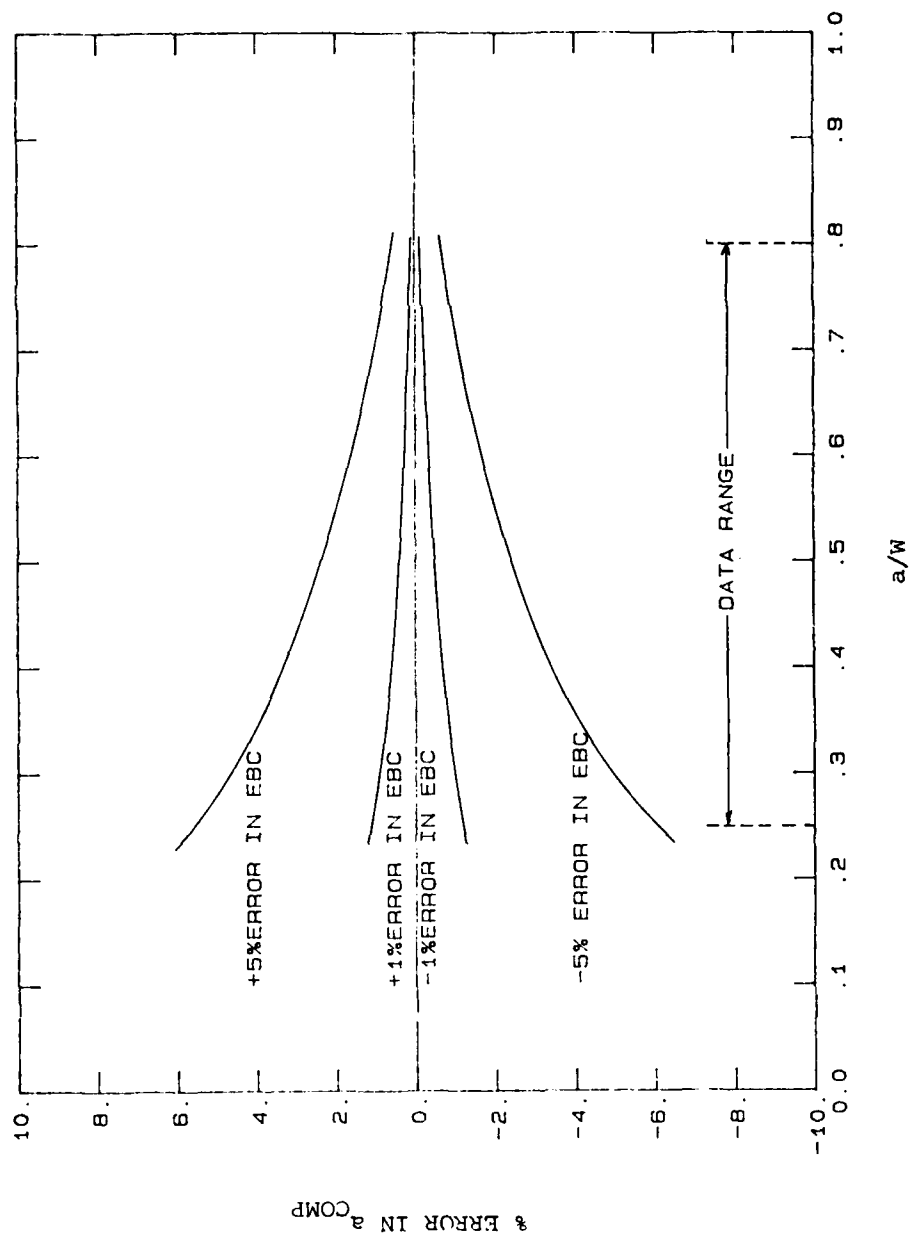
17

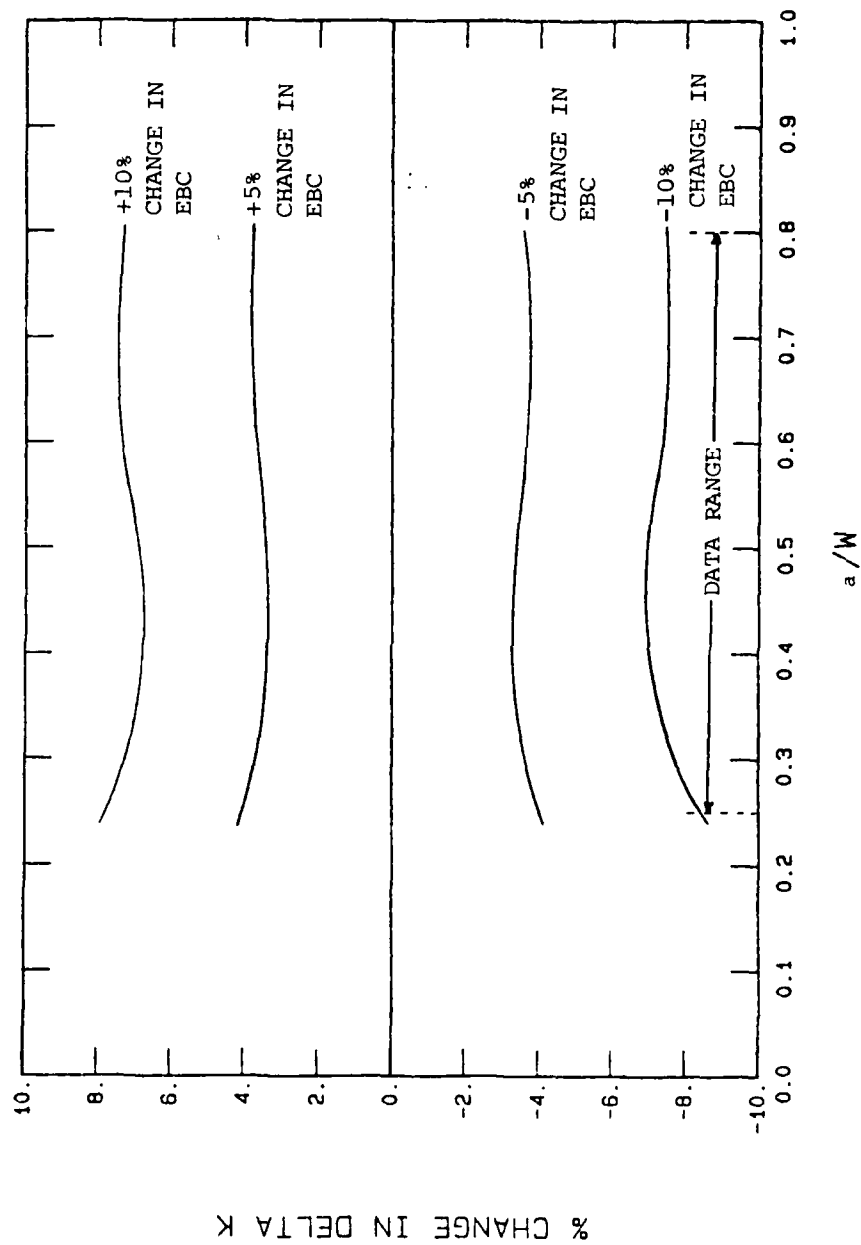Figure 6.   Effect of Errors in EBC on Compliance Calculated Crack Length.

18

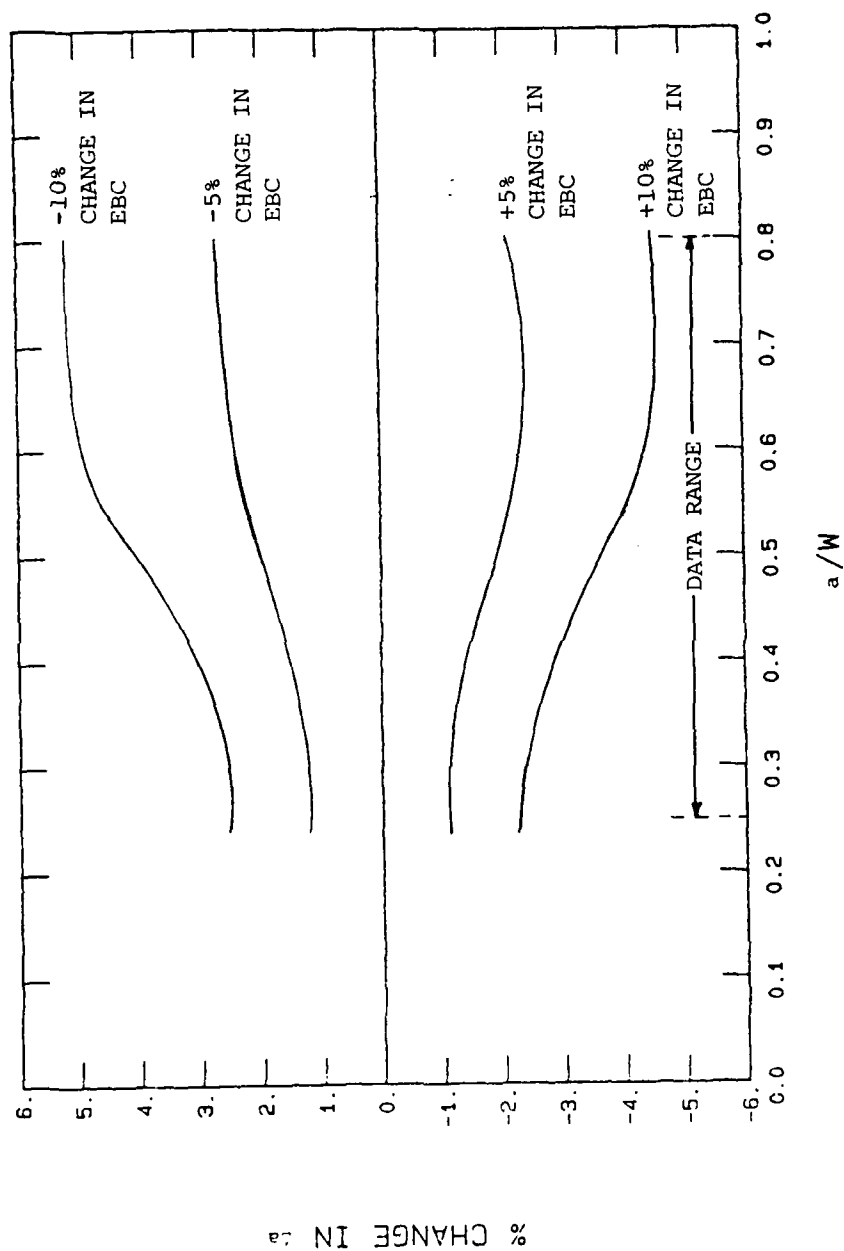Figure 7. Percent Change in ΔK as a Function of Change in EBC.

Figure 8. Percent Change in Δa as a Function of Change in EBC.

20

results produced curves which approximate the errors associated with experimental increments. It can be seen from Figure 8, that a systematic (percent) error in EBC will result in a systematic percent error in Δa which is opposite in sign and which is upper-bounded at about one-half of the error in EBC. The absolute value of the percent errors in Δa are noted to gradually increase throughout the crack length range of interest for a fixed percent error in EBC. The reason that the percent errors in Δa are opposite in sign to the percent errors in EBC can be obtained using Figure 6, where it is observed that the gradient of crack length error relative to crack length is negative.

Figures 6 through 9 were found to be very helpful in focusing on the reasons for apparent errors in crack growth rate behavior. Before addressing how the above information can be utilized to bring compliance established crack growth rate behavior in line with visual behavior, we wish to consider the potential causes for error in the factors involved in the EBC product.

4.3 AN ASSESSMENT OF POTENTIAL ERRORS

There can be both systematic and random errors in measuring and using compliance to calculate the crack growth rate behavior. This subsection will identify an attempt to quantify the systematic and random errors relative to their effect on crack growth rate behavior of a single specimen. The random errors will be considered first.

The primary random error that could cause problems with compliance based crack growth rate behavior is the result of the measurements of compliance based on determining the inverse slopes of successive load-displacement curves. Compliance (C) values were determined from the slopes of lines that were visually fitted to the upper linear portion of the load-displacement curves. The errors associated with this measurement procedure would result in random errors in the compliance calculated
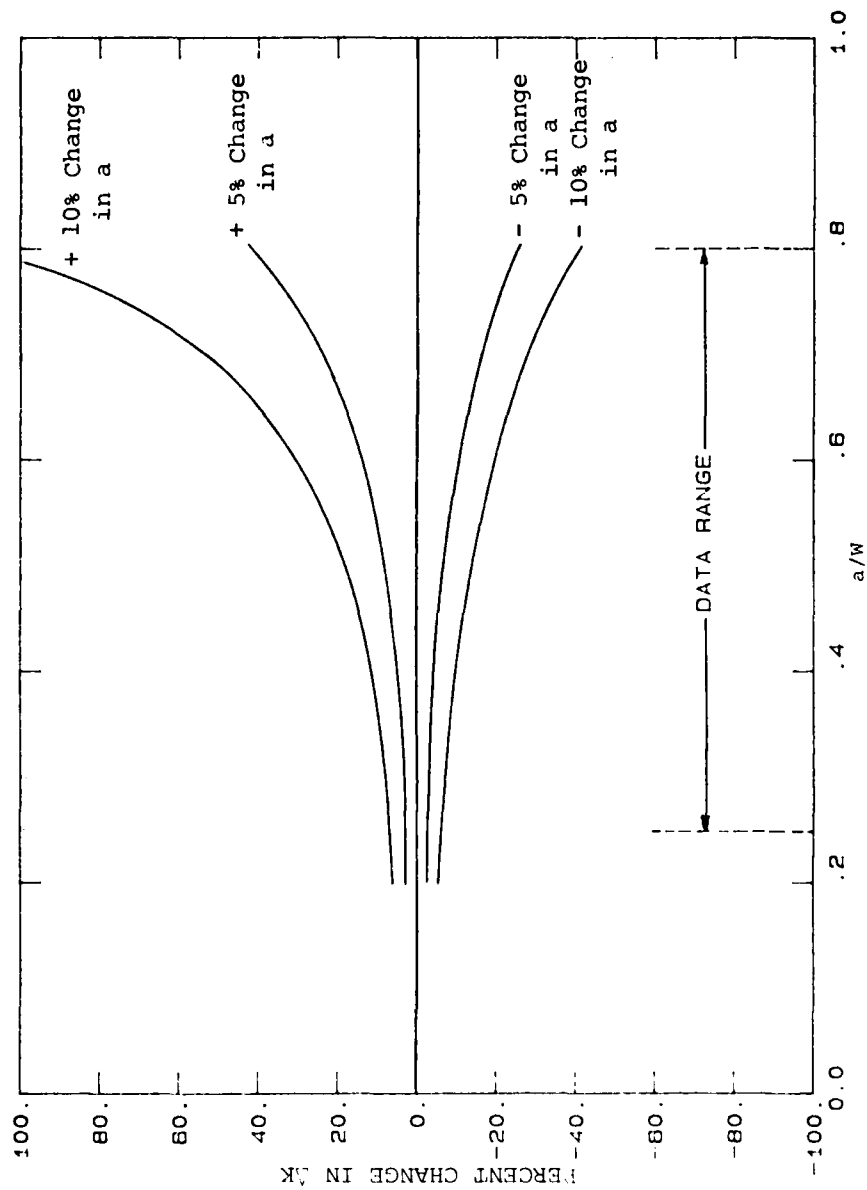
21

Figure 9. Percent Change in ΔK as a Function of Change in Crack Length.

22

crack lengths and in random behavior about nominal crack growth
rate curves. These errors would not produce a general offset
of a specimen's crack growth rate behavior as established by
compliance and by visual methods, as was illustrated in Figure 5.

There are a number of potential systematic errors which
could directly influence the error in EBC and the resulting crack
growth rate behavior. There could be errors in the measurements
of specimen geometry and of the location of the displacement gage.
Errors could exist in both the calibration of the load-displace-
ment measurement system and in the assumption whereby a constant
value of elastic modulus (E) was used for all specimens indepen-
dent of the heat treatment received. The magnitude of each of
these errors are considered in turn.

The geometric measurements of specimen height, width,
and thickness can all be determined to within ± 0.001 inches.
The most significant error would be that of thickness and it
would produce an error of less than ± 0.5 percent in EBC for all
the specimens tested in this program. This error in EBC would
produce a negligible error in compliance calculated crack lengths,
based on the analysis presented in Figure 6. The projected error
in the resulting crack growth rates and stress-intensity factor
range would also be negligible for such thickness errors.

Errors associated with the actual displacement (COD)
measurement location can result in systematic errors in compliance
(C). In this investigation, the COD-measurement location was the
integrally machined knife-edges on the front face of the specimen,
0.500 inches to the right of the loading line shown in Figure 2
for a specimen width (W) of 2.000 inches. This measurement
location corresponds to a location parameter value (X/W) of
-0.250 relative to the Hudak et al.[4] scheme of COD measurement
location. An X/W = 0 corresponds to the loading line. An upper
bound on error in (X/W) was estimated to be ± 2 percent for the
set of sixteen specimens.

Using the wide-range elastic compliance expression for compact tension specimens[4], the value of a/W was calculated for the various values of X/W using EBC values from 20 to 400. Figure 10 shows that the resulting plots of a/W versus X/W are nearly linear. Therefore, we use an approximate relationship between a/W and X/W, i.e.,

$$a/W = \left(\frac{a}{W}\right)_0 + \frac{(a/W)_0 - (a/W)_{-.250}}{0 - (-.250)} \left(\frac{X}{W}\right) \qquad (4)$$

to describe each of the curves shown in Figure 10. The effect of the error in the COD-measurement location (X/W) upon a/W, was evaluated by substituting -0.255 and -0.245 in Equation 4 for each EBC curve given in Figure 10. The results of the error evaluation are presented in Figure 11. As shown, it was determined that the error in crack length ranged from approximately 1 percent at a/W equal to 0.25 to less than 0.1 percent at a/W equal to 0.8. The error in ΔK resulting from the error in COD-measurement location would be approximately 0.4 percent over the entire range of a/W from 0.25 to 0.8. Thus, the COD-measurement location had little effect on growth rate curves and would not produce the magnitude of general offsets observed in Figure 5.

The cumulative errors in the load-displacement system were estimated in Section 2 to result in about a five percent maximum error in compliance for any one load-displacement measurement. As also indicated in Section 2, part of this error is due to calibration of the equipment (load cell, displacement gage, x-y recorder, etc.) and part of this error is due to the graphical measurement of the slope of the load-displacement curve. If one isolates the systematic errors associated with calibration, the measurement system might result in a maximum of three percent error in compliance. An error of three percent in compliance is more than sufficient to cause an offset in the compliance determined fatigue crack growth rate behavior.
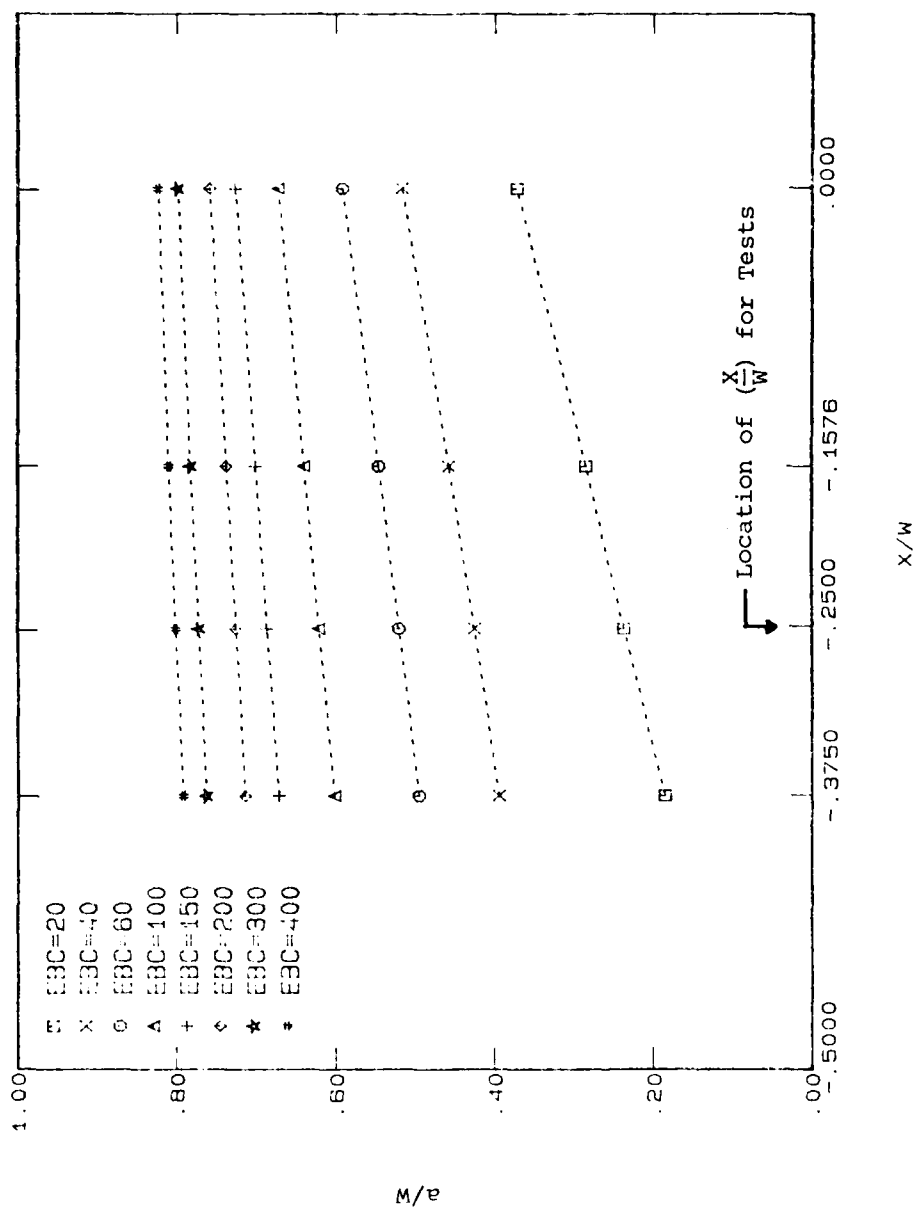
Figure 10.   Relationship Between Compliance Determined a/W and COD Measurement
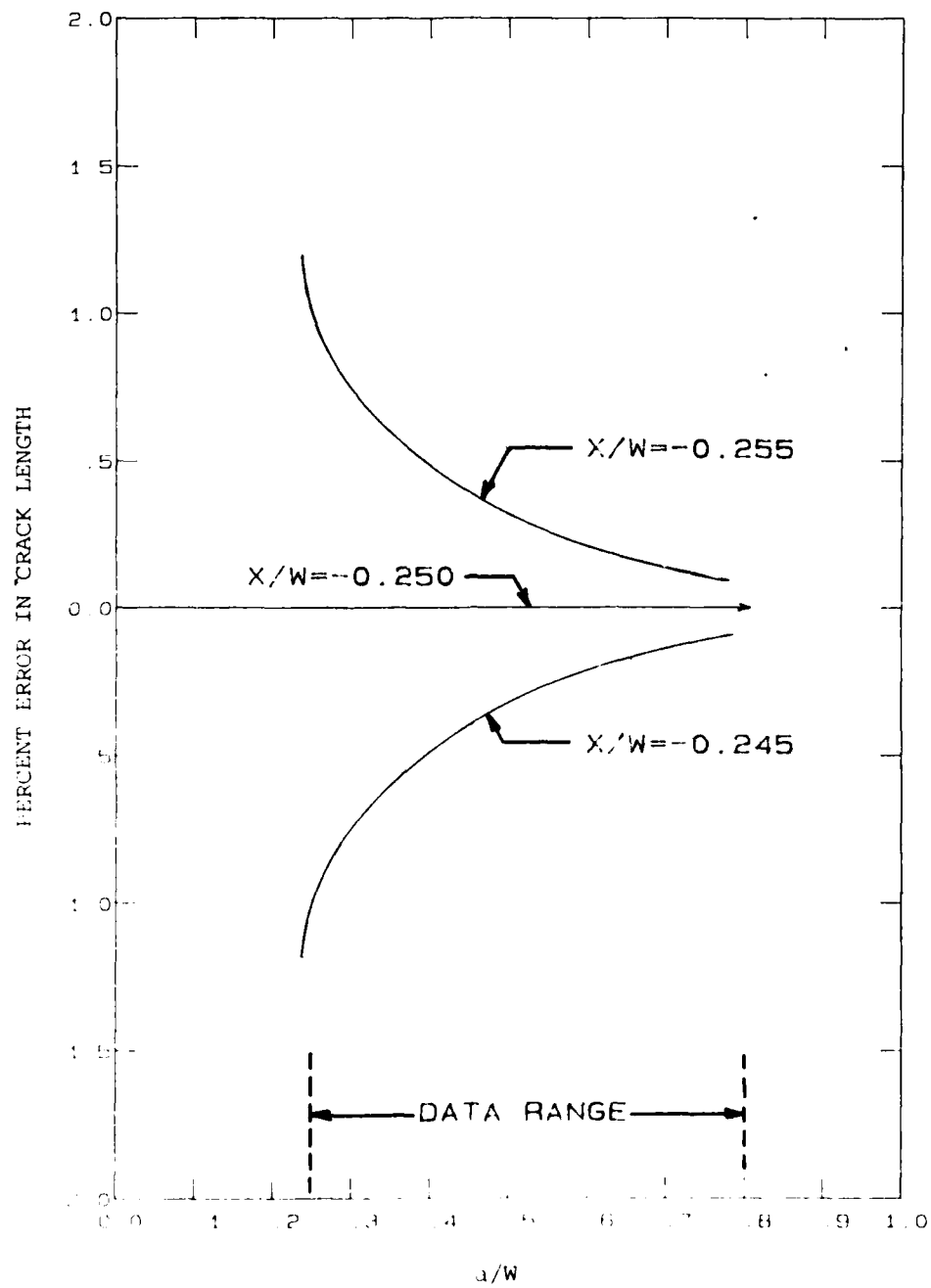Location (X/W) for EBC Ranging From 20 to 400.

25

Figure 11.   Percent Error in Crack Length Associated with an Error
in the Crack-Opening-Displacement Measurement Location.

26

Another systematic error which may occur in the calculations of crack growth rate behavior is the error in assumption of the elastic modulus (E) as a constant. In Section 2, the elastic modulus was assumed to be represented by a handbook value of $E = 10.6 \times 10^6$ psi. This assumption could be clearly in error for the 7091 powder aluminum alloys considered in the test program. This material was subjected to a wide range of processing and heat treatment conditions and exhibited substantial scatter in the yield strength property as shown in Table 1. The variance in elastic modulus is given by one-half the variance in yield strength, i.e., if E varies by ± 3 percent, then it can have a substantial impact on the estimates of EBC and thus crack growth rate behavior.

The systematic errors associated with the compliance system and with the assumption of elastic modulus are basically coupled since it is not practical to conduct tensile tests on all crack growth rate test specimens (in order to accurately estimate the elastic modulus). However, because the two types of errors can be coupled with the product EBC used to estimate crack growth behavior, it is relatively easy to develop a procedure which minimizes the total systematic error for any given test.

4.4   DATA REDUCTION USING AN EFFECTIVE MODULUS

One method of evaluating the potential effect of coupled errors in compliance and elastic modulus is to utilize the inverse representation of Equation 2 which expresses compliance as a function of crack length. The dimensionless compliance (EBC) for the compact tension specimen was given by Hudak et al.[3] as:

$$EBC = (1 + \frac{0.25}{\cdot}) \; (\frac{1+}{1-})^2 \; (1.61369 + 12.6778 \cdot$$

$$\tag{5}$$

$$-14.2311 \cdot^2 - 16.610 \cdot^3 + 35.0499 \cdot^4 - 14.49432 \cdot^5)$$

where α = a/W. If measured values of crack length and compliance are utilized in conjunction with Equation 5, then an effective modulus (E_{eff}) can be derived from each specimen. The effective modulus replaces the elastic modulus (E) in Equation 5 and provides an absolute equality for measured values of visual crack length ($a_{Reference}$) and the compliance at this $a_{Reference}$. The calculated effective modulus values and the visual crack lengths ($a_{Reference}$) for the 16 specimens are presented in Table 3. The average effective modulus was 11.06 x 10^6 psi with a standard deviation of 0.69 x 10^6 psi for the set of 16 specimens. Table 3 also lists the ratio of the effective modulus to the handbook modulus ($f = E_{eff}/E$) for each specimen. The effective modulus is seen to range from about 14 percent higher to a 9 percent lower than the handbook value, with a mean offset which is about 4 percent high. Effective modulus values were calculated at other crack lengths where compliance measurements were available and the results were somewhat similar to those given in Table 3. It was then decided to utilize the Table 3 effective modulus values in place of the handbook modulus for calculations of crack length based on Equation 2.
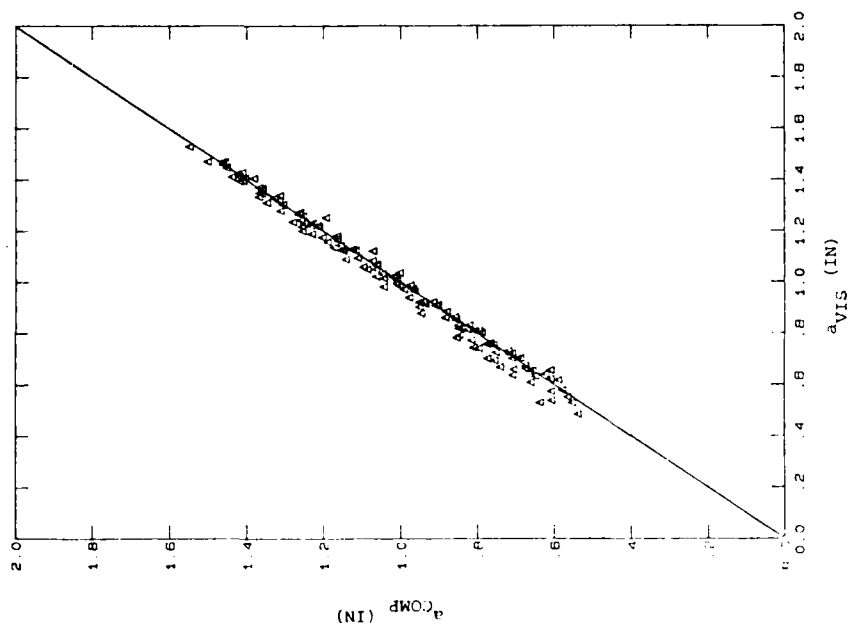
Figure 12 shows the visual crack length versus the compliance calculated crack length using a "handbook" modulus of 10.6 x 10^6 psi for the set of 16 specimens and using Table 3 effective modulus value calculated from a known crack length for each of the 16 specimens. The use of the calculated effective modulus values has significantly consolidated the data, resulting in better correlation between the visual crack length and the compliance calculated crack length over the full range of crack lengths.

As a specific example of the improvement in crack length determination resulting from using the effective modulus is shown in Figure 13. Not only does the effective modulus improve the accuracy of the determination near the crack length at which the effective modulus is calculated, but it improves the accuracy throughout the crack length range of interest.

28

TABLE 3

EFFECTIVE MODULUS VALUES

Specimen Number	[a]Reference	E_{eff} Effective Modulus (psi x 10^6)	$f = \dfrac{E_{eff}}{E^*}$
CTX4	.6074	12.01	1.133
CTX32	.9921	11.11	1.048
CT331	.8501	11.29	1.065
CT472	.5387	11.66	1.100
FC41	.6095	11.25	1.061
FC42	.6737	10.86	1.025
FC61	.7651	10.73	1.012
FC71	.5533	11.05	1.042
FC91	.6095	10.37	0.978
SMA1	.5896	10.12	0.955
SME	.7090	11.93	1.125
SM1TF	.6545	12.07	1.139
SM3TF	.6231	9.70	0.915
SM6TF	.5661	10.88	1.026
SM8TF	.6083	11.54	1.089
SM8TS2	.6087	10.41	0.982
	Mean =	11.061	1.043
	Standard Deviation =	0.692	0.0653
	Coefficient of Variation =	6.26%	6.26%

$E = 10.6 \times 10^6$ psi
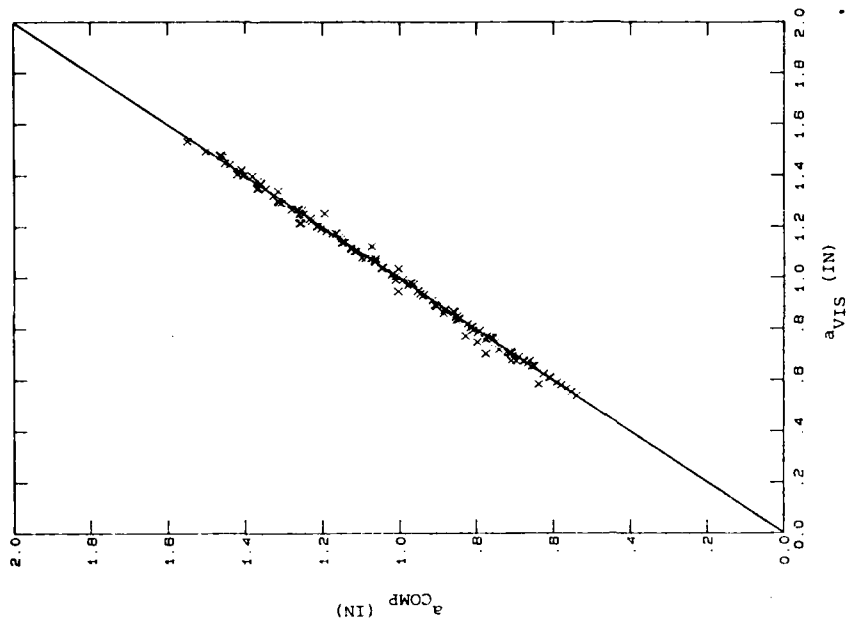
Compliance Calculated Crack Length Versus
Visual Crack Length Using a Modulus Value
Calculated from a Known Crack Length for
Each of 16 Specimens.

Compliance Calculated Crack Length Versus
Visual Crack Length Using a Handbook Modulus
Value of 10.6 x 106 psi for the Set of 16
Specimens.

Figure 12. Compliance Calculated Crack Length Versus Visual Crack Length Using
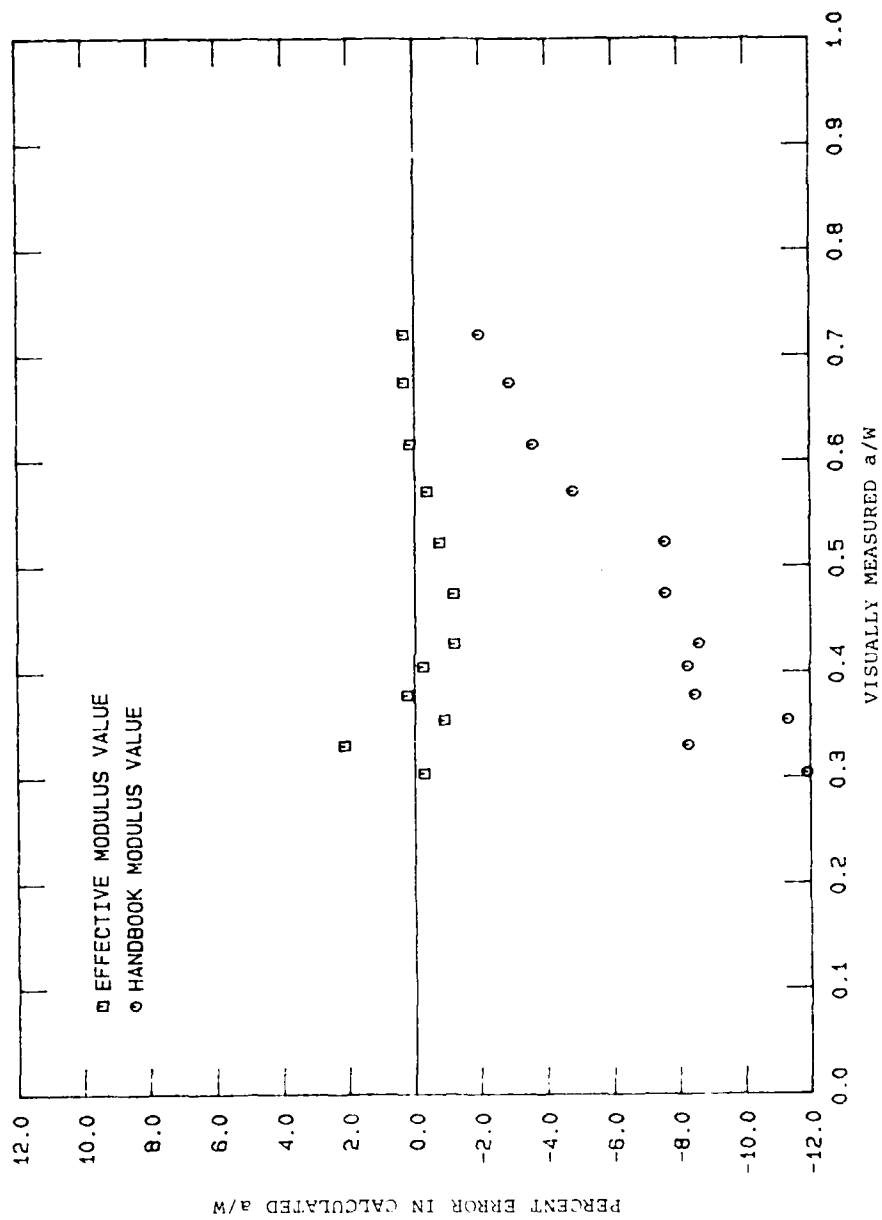a Handbook Modulus Value and a Calculated Modulus for the Set of 16
Specimens.

Figure 13. Percent Error in Calculated a/W as a Function of Measured a/W.

31

The data presented in Figure 5 indicate that the trend
of the compliance calculated crack growth rates based on the
"handbook" modulus are comparable to the visual crack growth
rates but offset from them. The major change in the compliance
determined crack growth rate curves when an effective modulus
is used instead of the "handbook" modulus is a shift in the
curves. The use of an effective modulus in EBC has an impact on
ΔK and Δa/ΔN calculations as shown by Figures 7 and 8,
respectively. A systematic percent error in EBC creates
approximately the same percent error in ΔK and about half that
percent error in the growth rate. The use of an effective
modulus for calculating crack length results in very good
correlation between the visual and compliance calculated data as
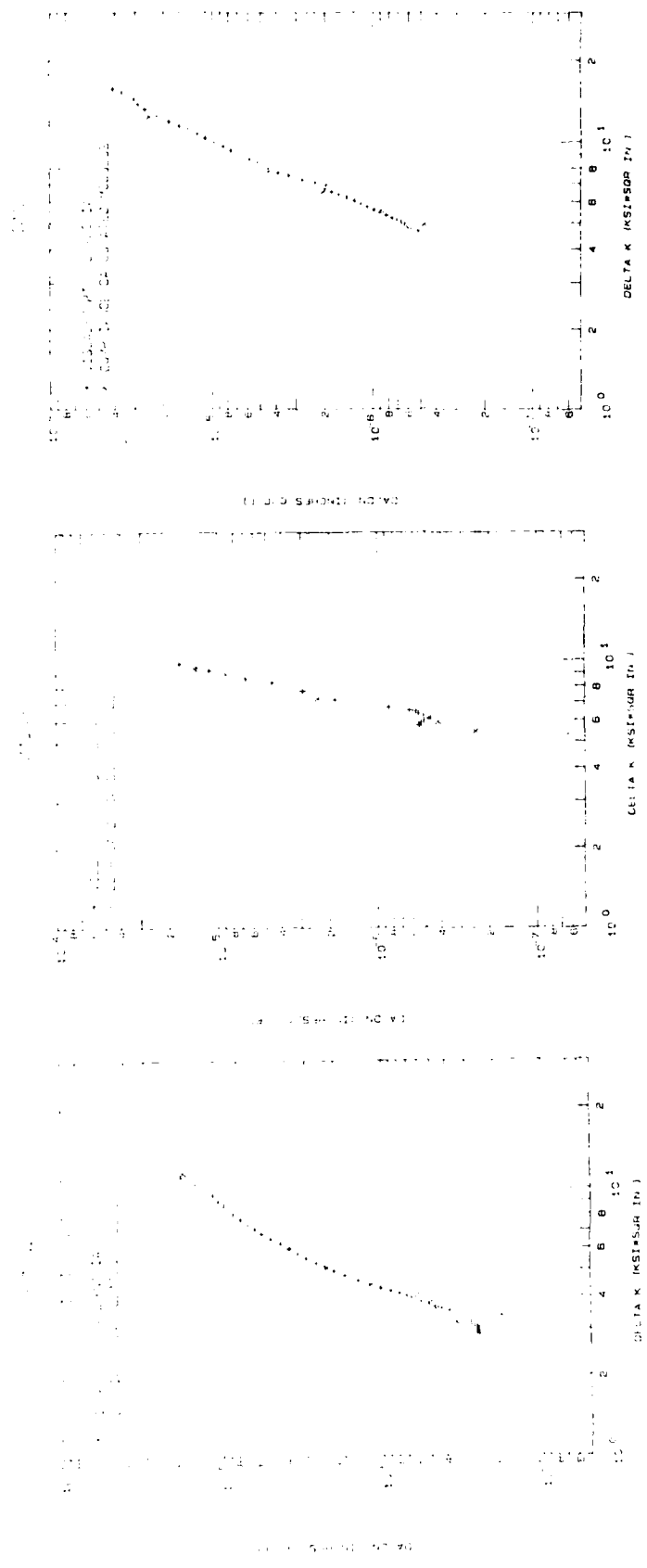presented in Figure 14.

Figure 14. Comparison Between Compliance Based Crack Growth Rates (Secant Method) and Visual Crack Growth Rates (7-Point Polynomial). Compliance Determined Crack Lengths Based on Elastic Modulus Adjusted for Individual Specimens.

33

SECTION 5
CONCLUSIONS AND RECOMMENDATIONS

Compliance is a viable method for measuring the fatigue crack length on a compact tension specimen. The use of compliance allows for automatic data acquisition, resulting in significant manpower savings, and increased testing time.

Compliance measurements must not be calculated from the minimum and maximum end points of the load-displacement curves. Closure or other factors may cause nonlinearity in the load-displacement curves and using the end points of the curve will result in erroneous compliance values which will result in erroneous crack length calculations. Compliance values must be determined from the linear portion of the load-displacement curve above any nonlinearity caused by closure or other factors.

The compliance value was determined from the loading portion of the load-displacement curve. Generally, the load-displacement curve exhibited little hysteresis and either the loading or unloading portion of the curve could have been used. The use of an effective modulus value could possibly compensate for any differences in compliance value between the loading and unloading portion of the load-displacement curve.

It is recommended that an initial visual crack length and an initial compliance value from the load-displacement curve be used to calculate an effective modulus value which can then be used over the full range of a/W values.

The tolerances for a compact tension specimen given in ASTM Test Method E647-81 allows considerable latitude in the specimen dimensions. If the crack-opening-displacement is being measured at the front face of the specimen and the specimen tolerances are taken to their limits, an error of up to 6.5 percent in the COD-measurement location (X/W) can occur. If X/W is maintained less than ± 2 percent, the ΔK values will have less than ± 0.5 percent error for 0.25 < a/W < 0.8.

The accuracy of fatigue crack growth rate versus ΔK calculated from compliance values is dependent upon the accuracy with which the absolute value of 'a' can be determined. The absolute value of 'a' is affected by the modulus value used in the compliance crack length calculation but the change in 'a' is relatively unaffected as long as the precision with which compliance is determined is constant. This indicates that the accuracy in Δa would be good even though the absolute value of 'a' could be in error.

For optical measurements, ASTM Test Method E647-81 requires a technique capable of resolving crack lengths of 0.004 inches or 0.002W, whichever is greater. For consistency between the compliance determined ΔK values and those determined from visual measurements, it is recommended that an effective modulus value be selected such that the compliance calculated crack length varies less than 0.004 inches from the actual crack length as determined visually. Equation 5 provides an easy and accurate method for determining the effective modulus within the accuracy suggested herein.

REFERENCES

1. Maxwell. D. C., "Fatigue Crack Growth Properties of Rapid Solidification Technique P/M Aluminum Alloy X7091," UDR-TM-81-38, University of Dayton, Dayton, Ohio, November 1981.

2. "Test Method for Constant-Load-Amplitude Fatigue Crack Growth Rates Above 10^{-8} m/Cycle," ASTM E647-81, Am. Soc. Testing Mats., 1981. Part 10 Annual Book of Standards.

3. Hudak, S. J., Jr., Saxena, A., Bucci, R. J. and Malcolm, R. C., "Development of Standard Methods of Testing and Analyzing Fatigue Crack Growth Rate Data," AFML-TR-78-40, Air Force Materials Laboratory, WPAFB, Ohio.

4. Saxena, Askok and Hudak, S. J., Jr., "Review and Extension of Compliance Information for Common Crack Growth Specimens," International Journal of Fracture, Vol. 14, No. 5, October 1978, pp. 453-468.

5. Yoder, G. R., Cooley, L. A., and Crooker, T. W., "Procedures for Precision Measurement of Fatigue Crack Growth Rate Using Crack-Opening Displacement Techniques," Fatigue Crack Growth Measurement and Data Analysis, ASTM STP 738, S. J. Hudak, Jr., and R. J. Bucci, Eds., American Society for Testing and Materials, 1981, pp. 85-102.

APPENDIX A

VISUAL AND COMPLIANCE DETERMINED
CRACK GROWTH RATE DATA

CTX32

Figure Al.   Comparison of Fatigue Crack Growth Rates of
             Specimen CTX32.
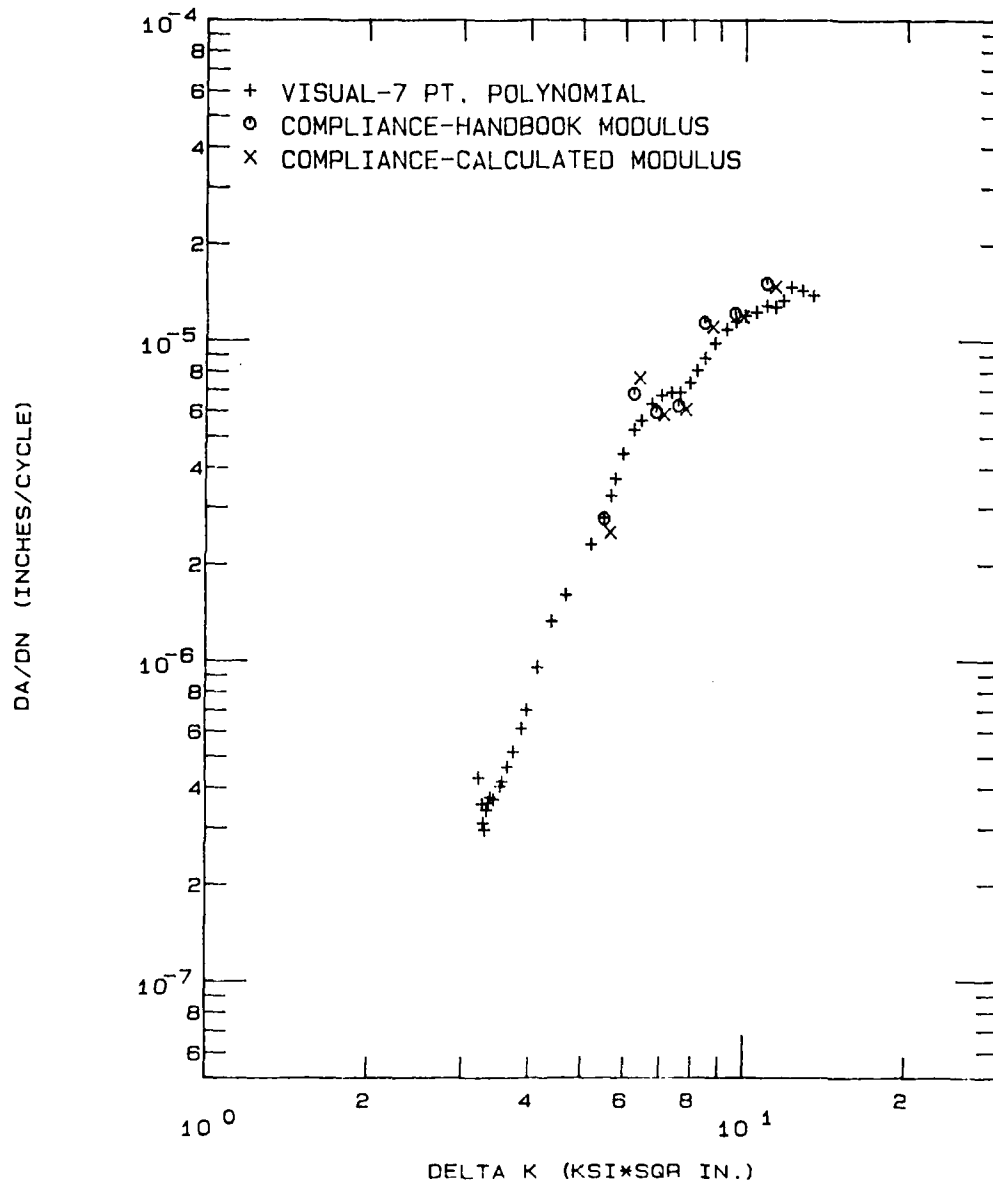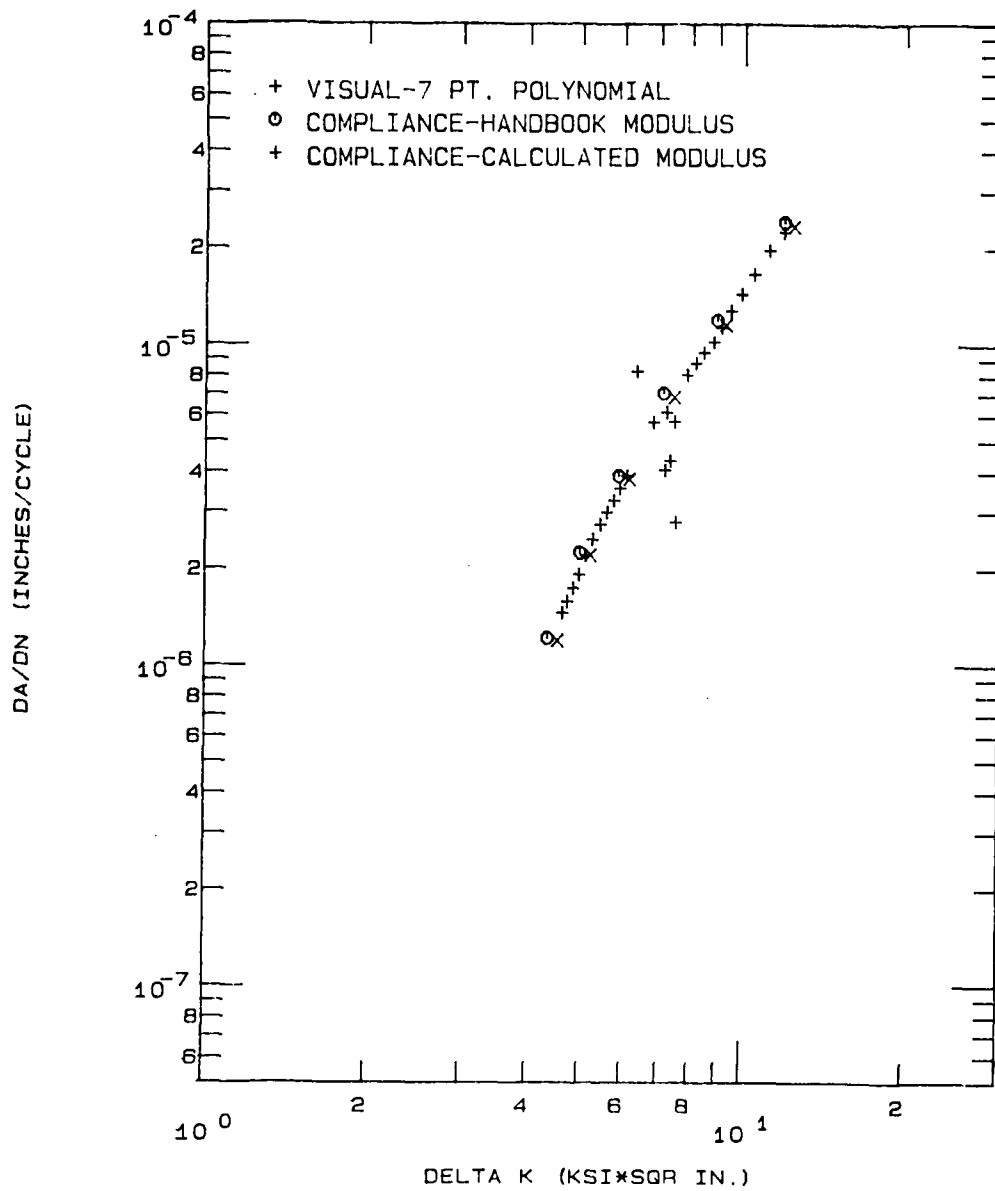
CT331

Figure A2. Comparison of Fatigue Crack Growth Rates of Specimen CT331.

39
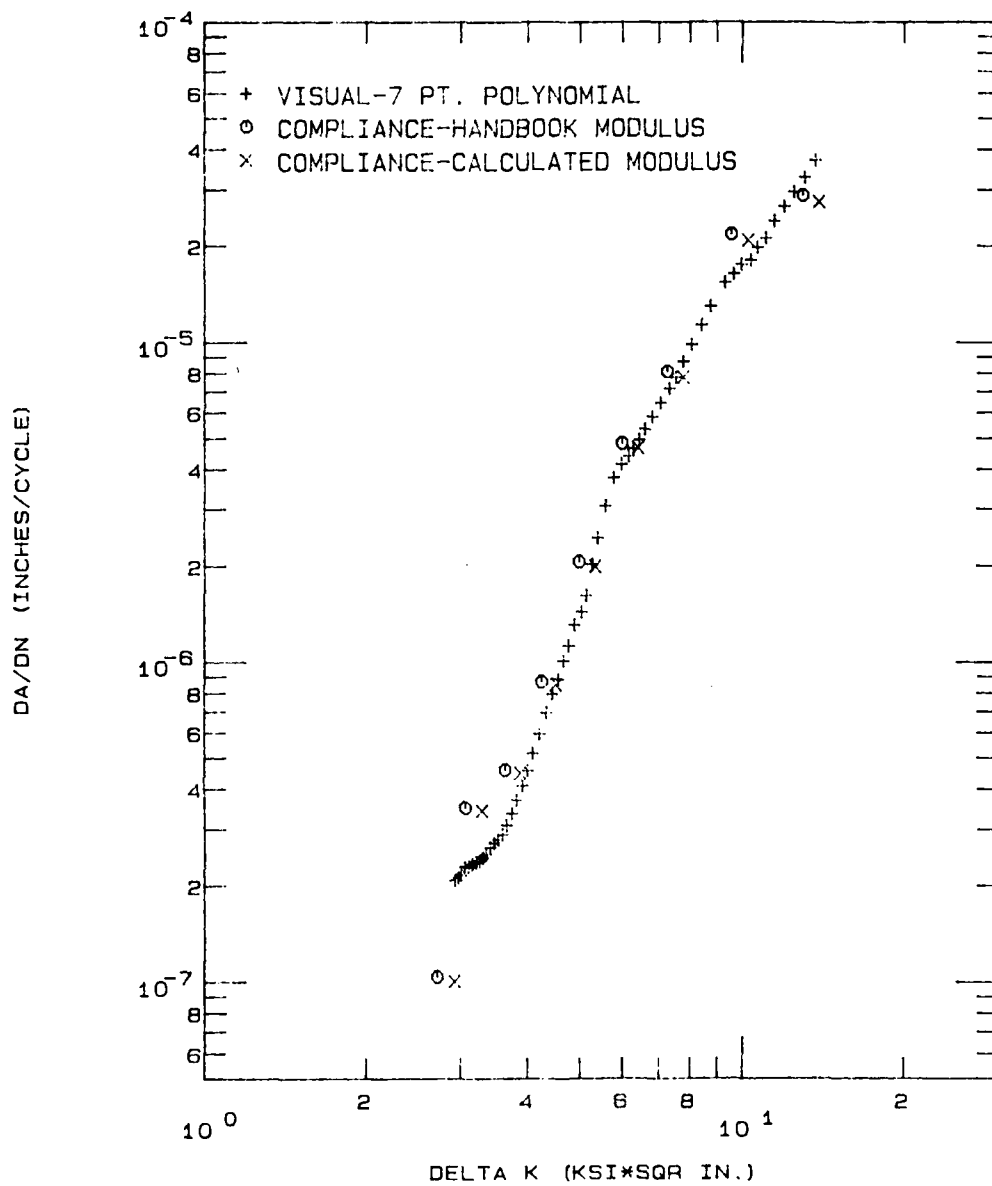
Figure A3.   Comparison of Fatigue Crack Growth Rates of
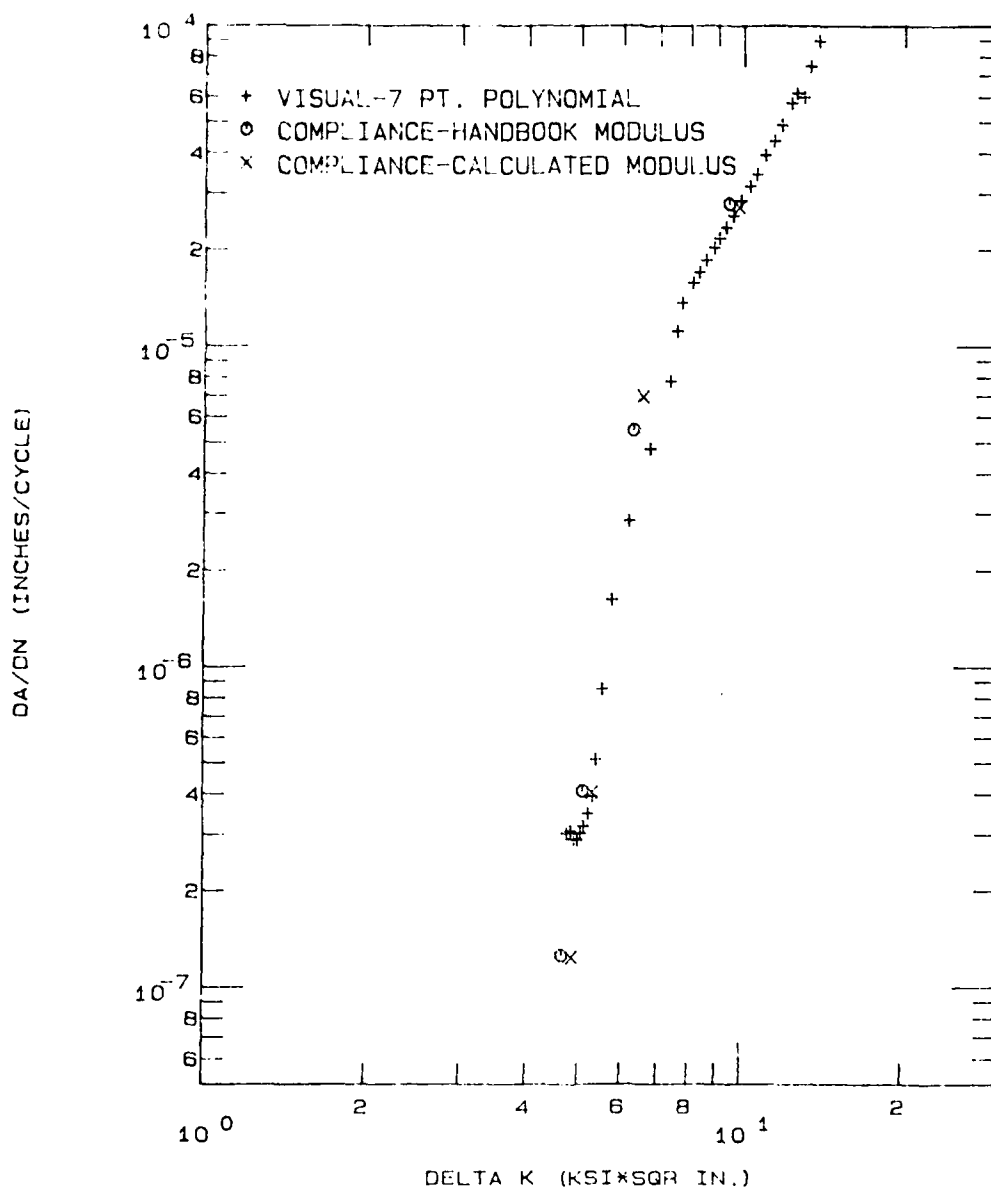   Specimen CT472.

FC41

Figure A4. Comparison of Fatigue Crack Growth Rates of
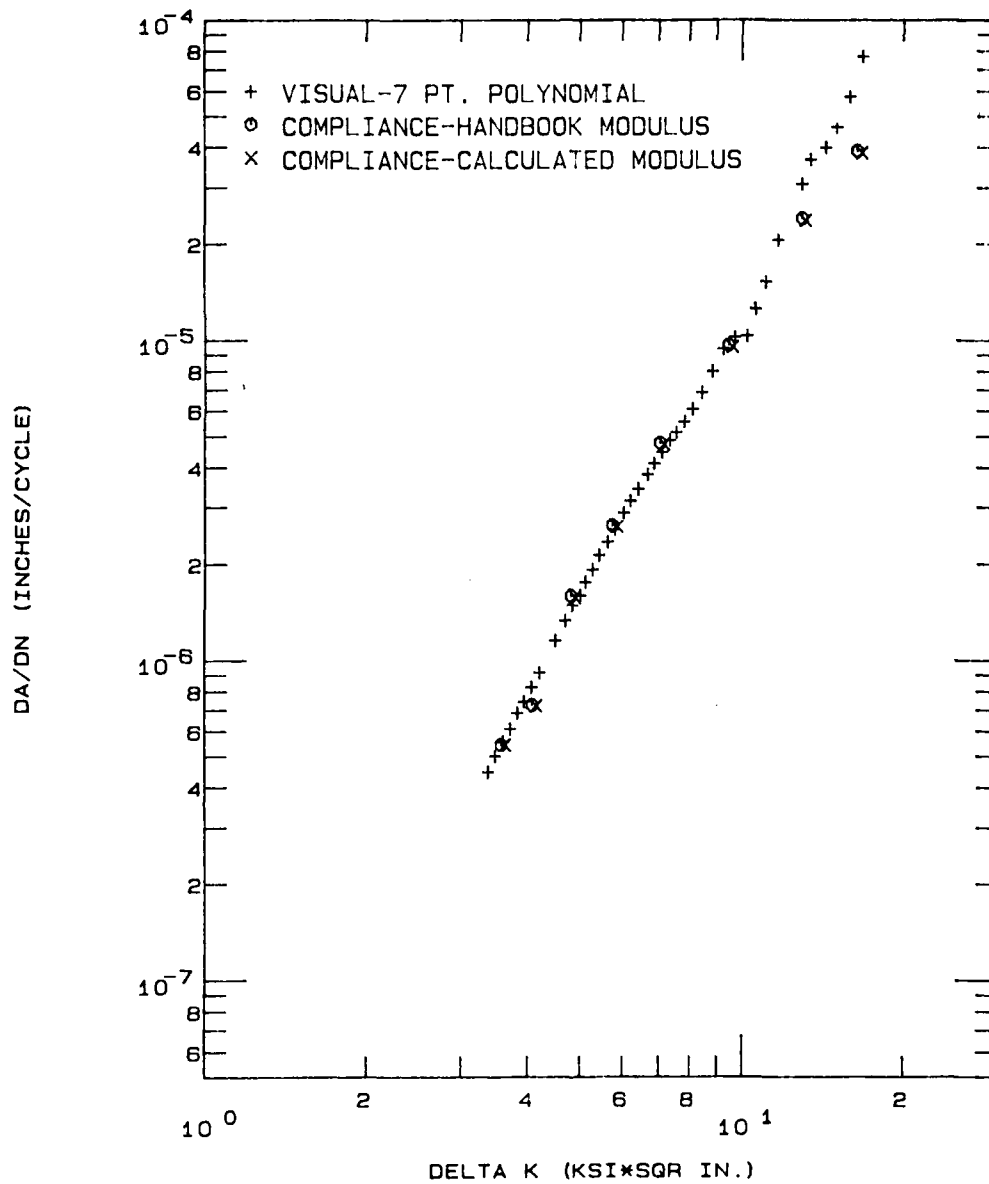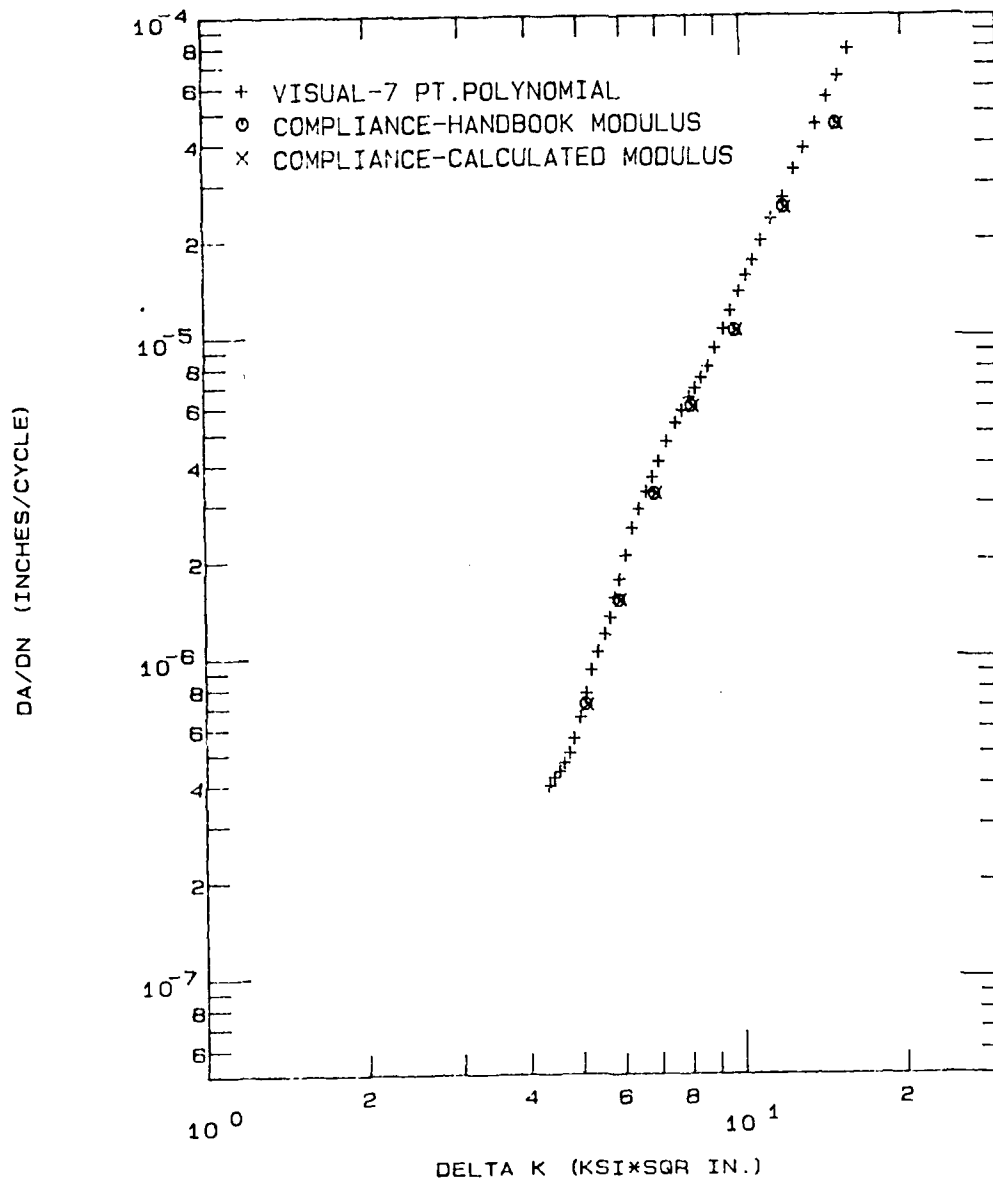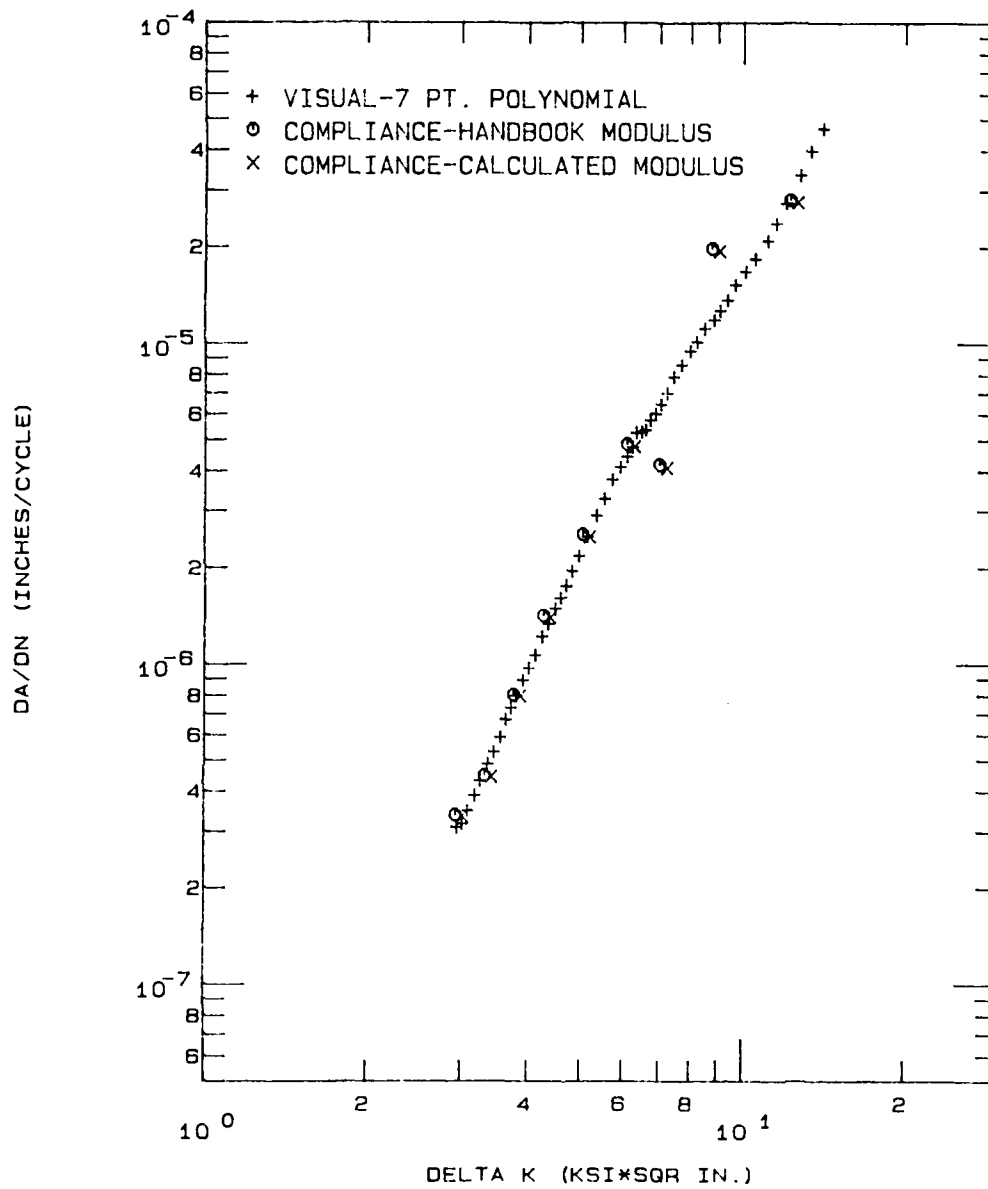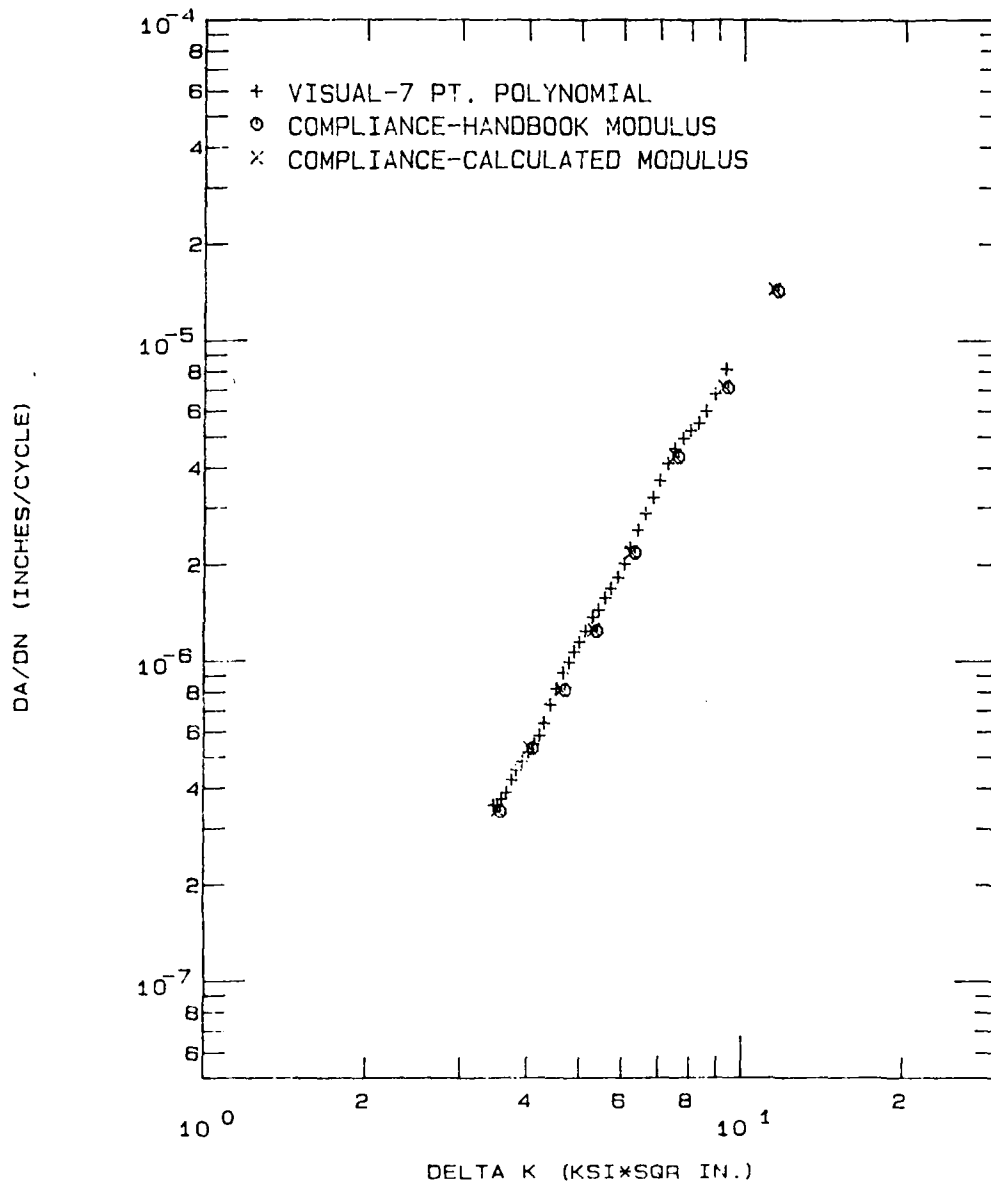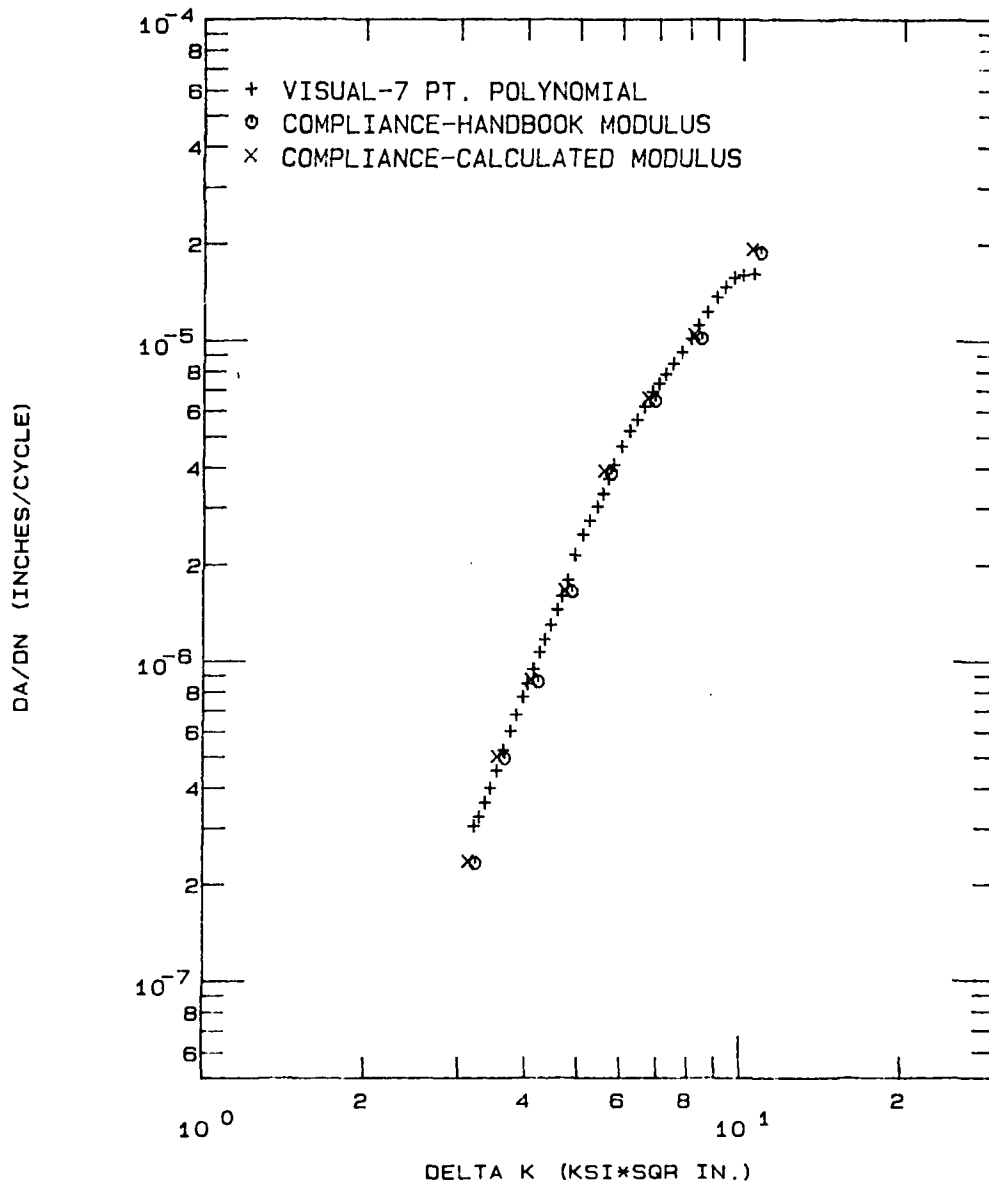   Specimen FC41.

FC42

Figure A5.   Comparison of Fatigue Crack Growth Rates of
             Specimen FC42.

42

Figure A6. Comparison of Fatigue Crack Growth Rates of Specimen FC61.

43

Figure A7. Comparison of Fatigue Crack Growth Rates of
Specimen FC71.

Figure A8.   Comparison of Fatigue Crack Growth Rates of
             Specimen FC91.

45

SMA 1

Figure A9. Comparison of Fatigue Crack Growth Rates of
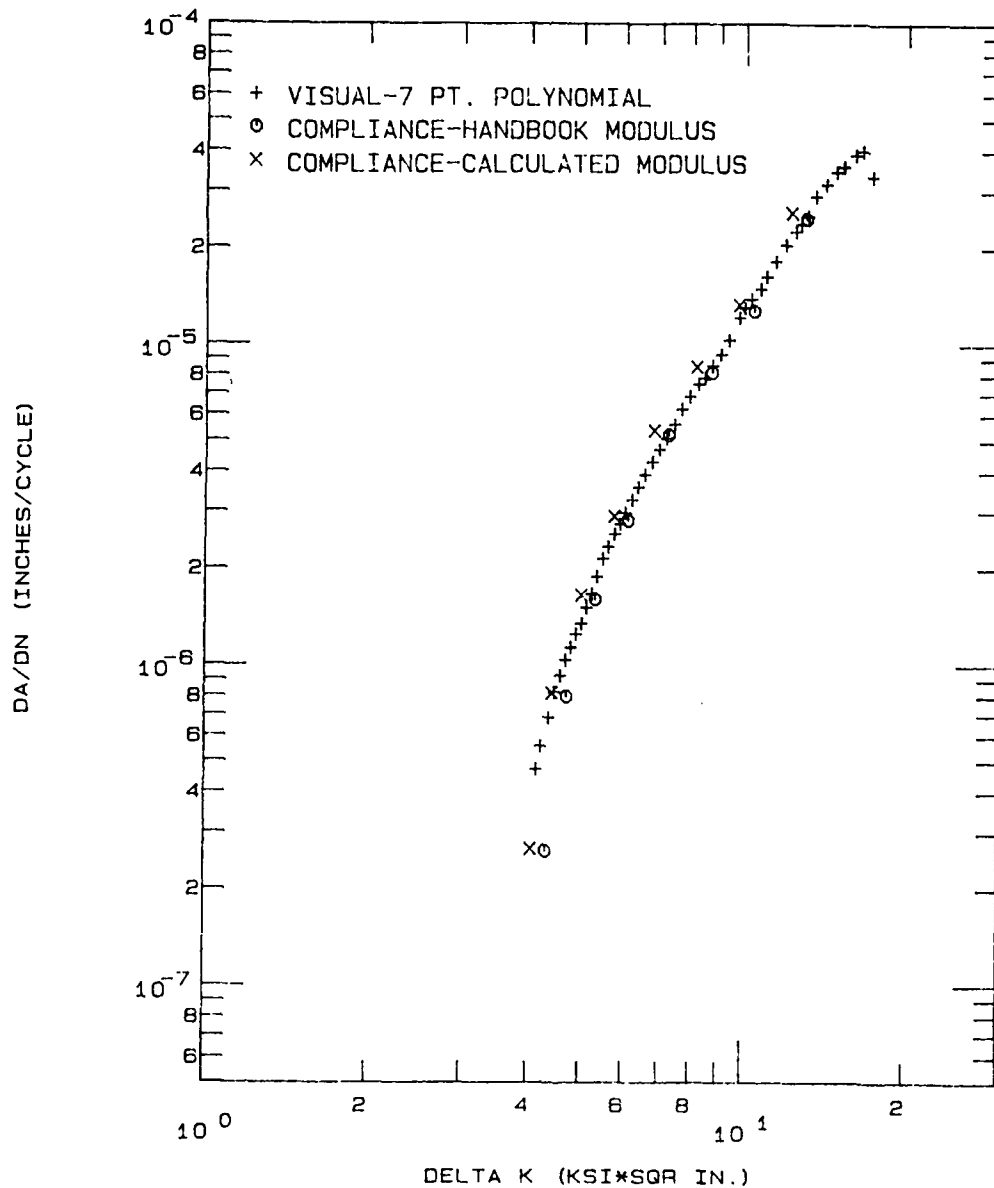   Specimen SMAl.

46

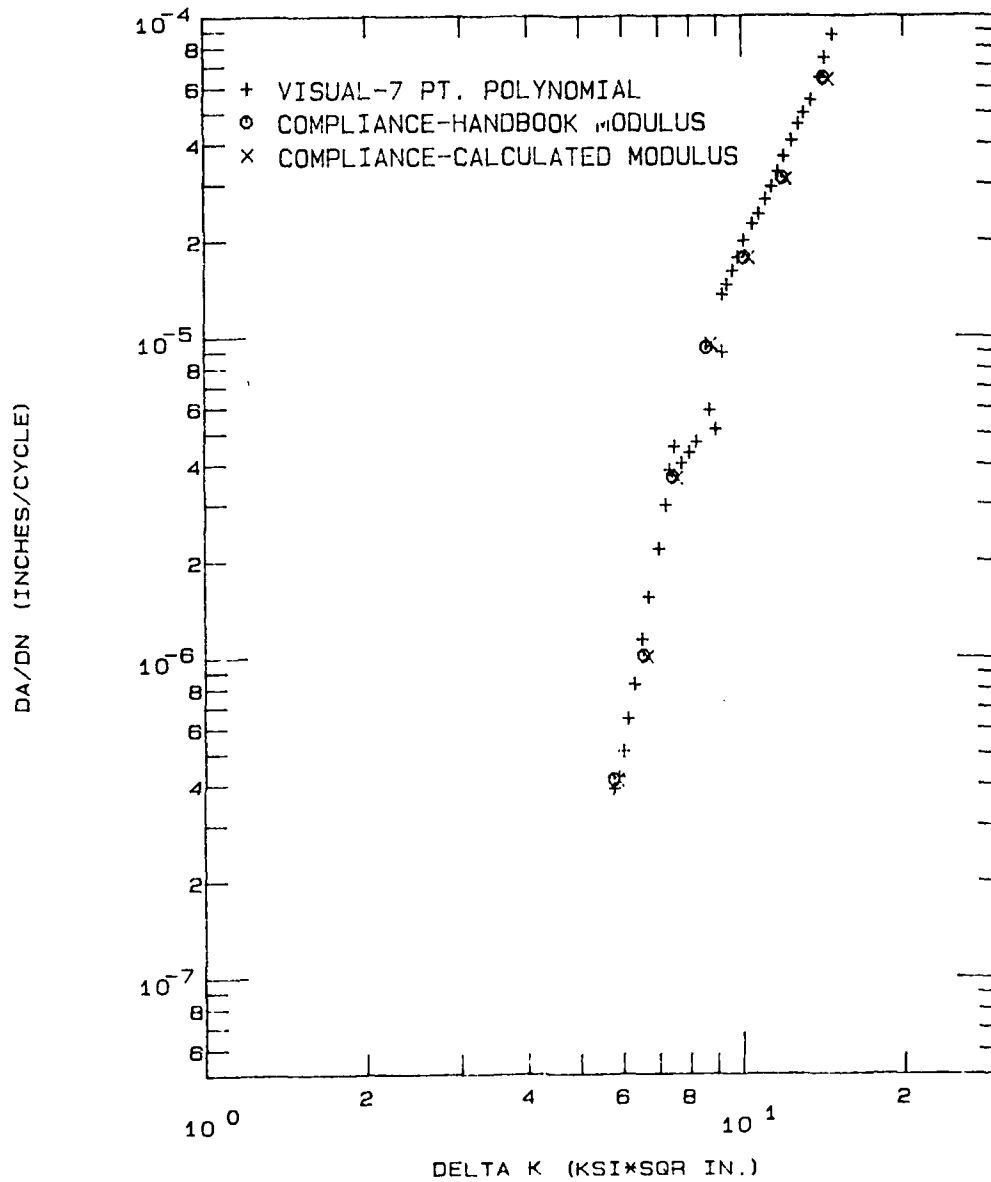Figure A10. Comparison of Fatigue Crack Growth Rates of Specimen SM3TF.

Figure All. Comparison of Fatigue Crack Growth Rates of
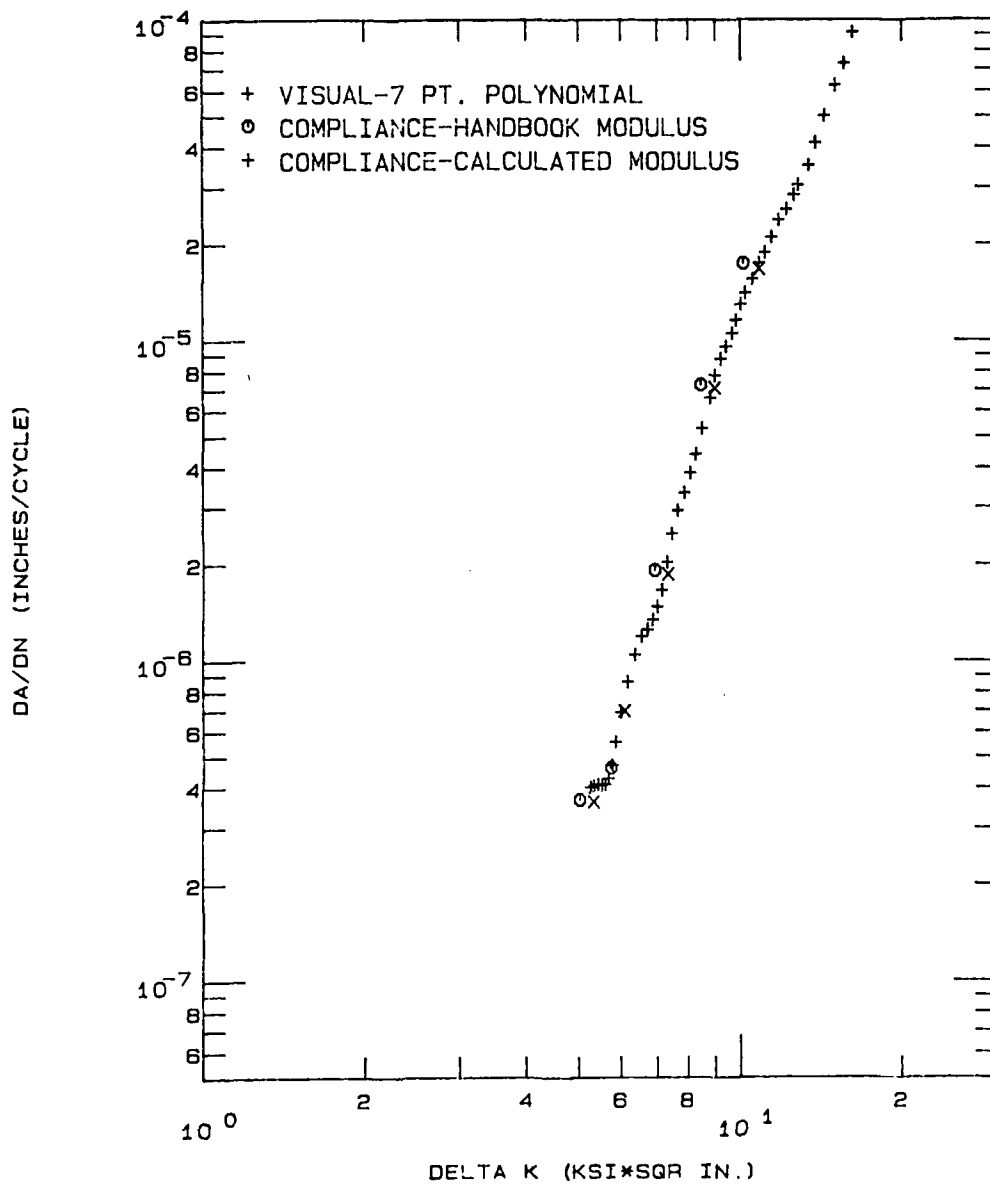Specimen SM6TF.

SM8TF

Figure A12. Comparison of Fatigue Crack Growth Rates of
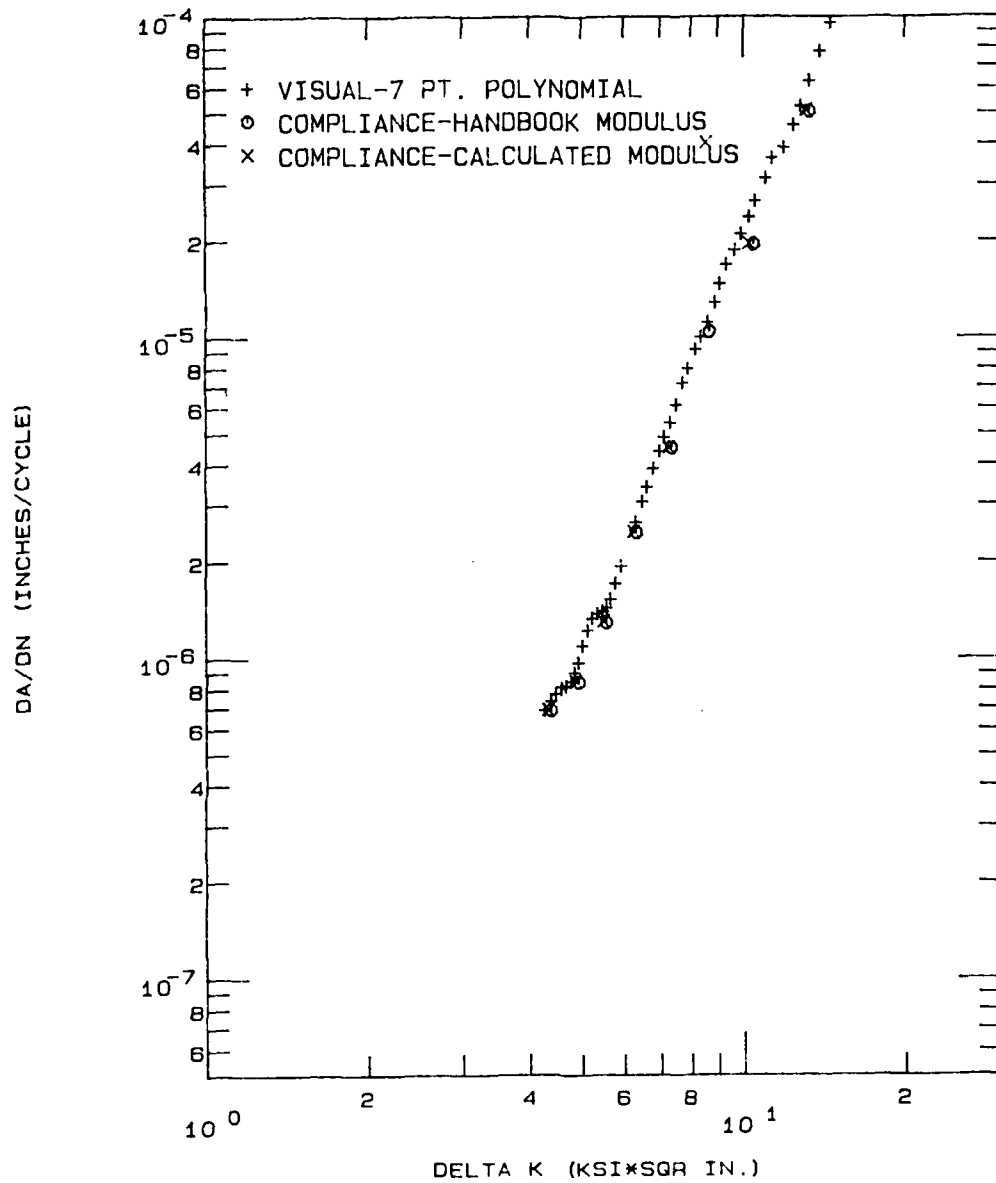Specimen SM8TF.

49

SM8TS2

Figure A13. Comparison of Fatigue Crack Growth Rates of
Specimen SM8TS2.

END

FILMED

9-84

DTIC